REGULATO[illegible] INFORMATION DISTRIBUTION [illegible]STEM (RIDS)

ACCESSION NBR:8405140448 DOC.DATE: 84/05/08 NOTARIZED: NO DOCKET #
FACIL:50-275 Diablo Canyon Nuclear Power Plant, Unit 1, Pacific Ga 05000275
AUTH.NAME AUTHOR AFFILIATION
SCHUYLER,J.O. Pacific Gas & Electric Co.
RECIP.NAME RECIPIENT AFFILIATION
EISENHUT,D.G. Division of Licensing

SUBJECT: Forwards errata to Attachment 7(b)-4 to Encl 7 (bending members - steel design current practice) of 840427 ltr re technical issues in License Condition 2.C.(II).Ack of matl receipt requested.

DISTRIBUTION CODE: B001S COPIES RECEIVED:LTR 1 ENCL 1 SIZE: 36
TITLE: Licensing Submittal: PSAR/FSAR Amdts & Related Correspondence

NOTES:J Hanchett 1cy PDR Documents. 05000275

	RECIPIENT ID CODE/NAME	COPIES LTTR	COPIES ENCL	RECIPIENT ID CODE/NAME	COPIES LTTR	COPIES ENCL
	NRR/DL/ADL	1	0	NRR LB3 BC	1	0
	NRR LB3 LA	1	0	SCHIERLING,H 01	1	1
INTERNAL:	ELD/HDS2	1	0	IE FILE	1	1
	IE/DEPER/EPB 36	3	3	IE/DEPER/IRB 35	1	1
	IE/DQASIP/QAB21	1	1	NRR/DE/AEAB	1	0
	NRR/DE/CEB 11	1	1	NRR/DE/EHEB	1	1
	NRR/DE/EQB 13	2	2	NRR/DE/GB 28	2	2
	NRR/DE/MEB 18	1	1	NRR/DE/MTEB 17	1	1
	NRR/DE/SAB 24	1	1	NRR/DE/SGEB 25	1	1
	NRR/DHFS/HFEB40	1	1	NRR/DHFS/LQB 32	1	1
	NRR/DHFS/PSRB	1	1	NRR/DL/SSPB	1	0
	NRR/DSI/AEB 26	1	1	NRR/DSI/ASB	1	1
	NRR/DSI/CPB 10	1	1	NRR/DSI/CSB 09	1	1
	NRR/DSI/ICSB 16	1	1	NRR/DSI/METB 12	1	1
	NRR/DSI/PSB 19	1	1	NRR/DSI/RAB 22	1	1
	NRR/DSI/RSB 23	1	1	~~REG FILE~~ 04	1	1
	RGN5	3	3	RM/DDAMI/MIB	1	0
EXTERNAL:	ACRS 41	6	6	BNL(AMDTS ONLY)	1	1
	DMB/DSS (AMDTS)	1	1	FEMA-REP DIV 39	1	1
	LPDR 03	2	2	NRC PDR 02	1	1
	NSIC 05	1	1	NTIS	1	1
NOTES:		1	1			

TOTAL NUMBER OF COPIES REQUIRED: LTTR 55 ENCL 48

PACIFIC GAS AND ELECTRIC COMPANY

PGandE 77 BEALE STREET • SAN FRANCISCO, CALIFORNIA 94106 • (415) 781-4211 • TWX 910-372-6587

J. O. SCHUYLER
VICE PRESIDENT
NUCLEAR POWER GENERATION

May 8, 1984

PGandE Letter No.: DCL-84-175

Mr. Darrell G. Eisenhut, Director
Division of Licensing
Office of Nuclear Reactor Regulation
U. S. Nuclear Regulatory Commission
Washington, D.C. 20555

Re: Docket No. 50-275, OL-DPR-76
Diablo Canyon Unit 1
License Condition 2.C.(II) - Errata

Dear Mr. Eisenhut:

On April 27, 1984, PGandE submitted Letter No. DCL-84-164 which summarized PGandE's actions for responding to each of the technical issues in License Condition 2.C.(II). Attachment 7(b)-4 to Enclosure 7 of that letter was incomplete. Enclosed is a complete Attachment 7(b)-4 to replace the one that was previously submitted.

Kindly acknowledge receipt of this material on the enclosed copy of this letter and return it in the enclosed addressed envelope.

Sincerely,

J. O. Schuyler

Enclosure

cc: J. B. Martin
H. E. Schierling
Service List

A001
1/0

PGandE Letter No.: DCL-84-175

ENCLOSURE

2

BENDING MEMBERS

STEEL DESIGN *CURRENT PRACTICE*

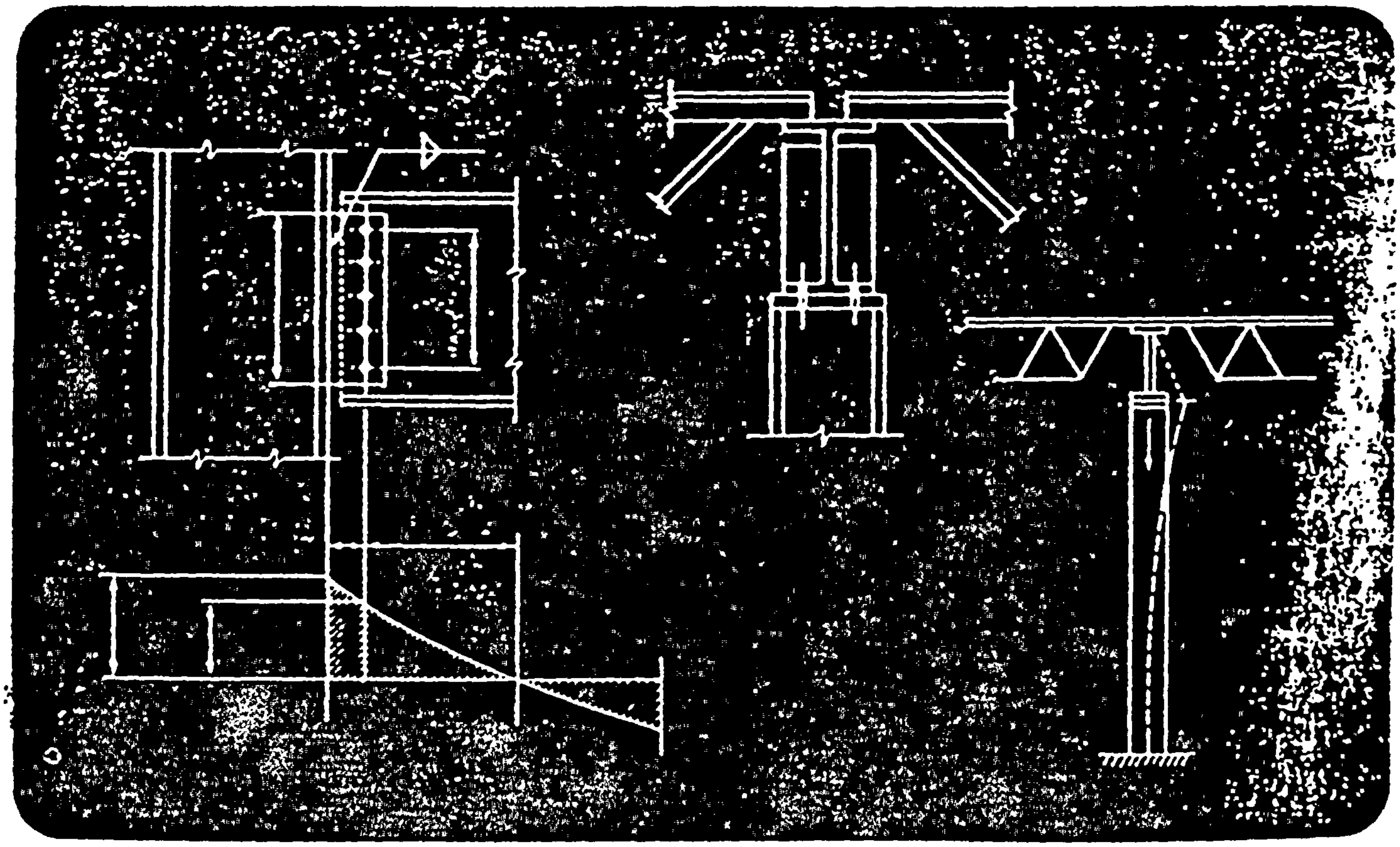

Slide No. 2-3

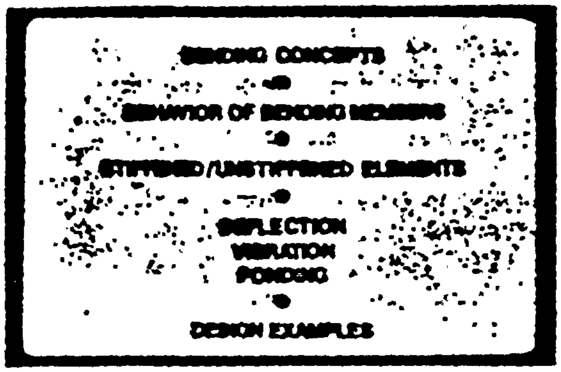

* Preview contents of the lecture.

* Bending concepts - review basic concepts.

* Behavior of Bending Members - related to different failure mode.

* Material includes:
  - compact sections
  - non-compact sections
  - laterally unsupported beams
  - box sections

Slide No. 2-4

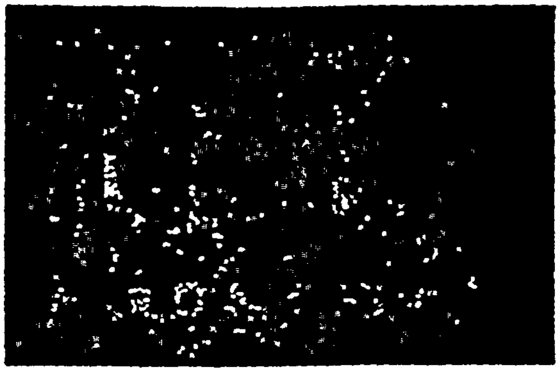

* Section modulus S = maximum moment from the moment diagram at working or design load levels divided by Allowable Bending Stress.

* Plastic modulus Z = maximum moment from moment diagram at some specified overload (usually 70% overload for gravity loads) divided by yield point.

* When are these formulas valid?

Slide No. 2-5

* To understand and properly utilize the design methods and specification provisions for structural steel design, the variables that affect beam behavior will be explored.

Slide No. 2-6

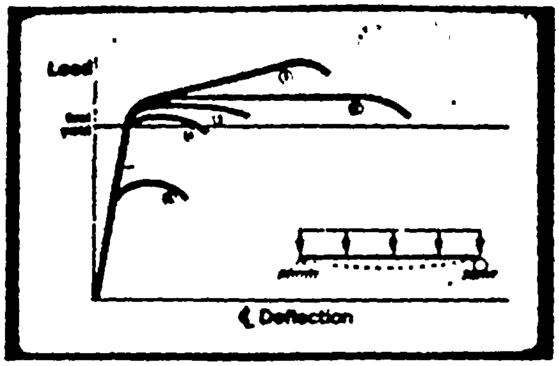

* All beam behavior cannot be represented by a single load-deflection curve because of the number of variables involved.

* Five curves represent potential behavior of a beam or girder in a building.

  - 1 2 Plastic straining without local or lateral buckling.
  - 3 4 Reach first yield without local or lateral buckling.
  - 5 Lateral or local buckling.

* The various allowable stresses permitted in the latest AISC Spec. are related to the behavior depicted in the 5 curves.

* Plastic Design is based on behavior curves (1) and (2) so provisions are established to prevent types (3) (4) (5).

* Curves 1 and 2 will generally provide the lightest beams but sometimes the fabrication and detail is increased because of the added bracing, stiffeners, etc.

* The proper design is the economical one, not the lightest one.

Slide No. 2-7

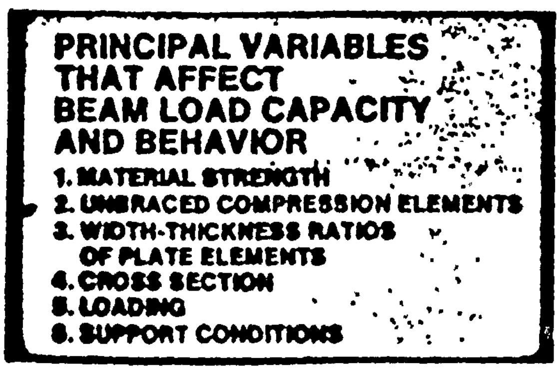

* Principal variables that affect beam load capacity and behavior.

Slide No. 2-8

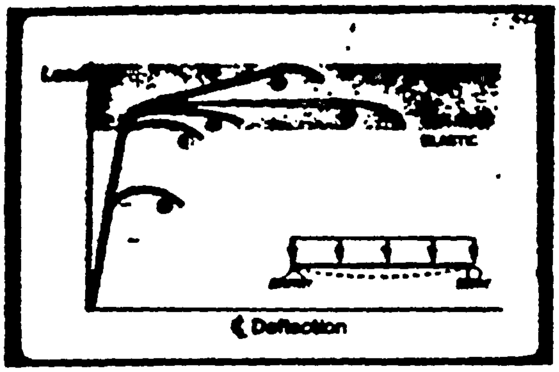

* Safe, economical structures can be designed on the basis of any one of these typical curves.

* Curves 1 and 2 will generally provide the lightest beams but sometimes the fabrication and detail cost is increased because of the added bracing, stiffeners, etc.

* The proper design is the economical one, not the lightest one.

* We will look at these curves in more detail and see how they relate to the latest AISC Spec. and Supplements.

* Of course, shear and deflection can also affect the design.

Slide No. 2-9

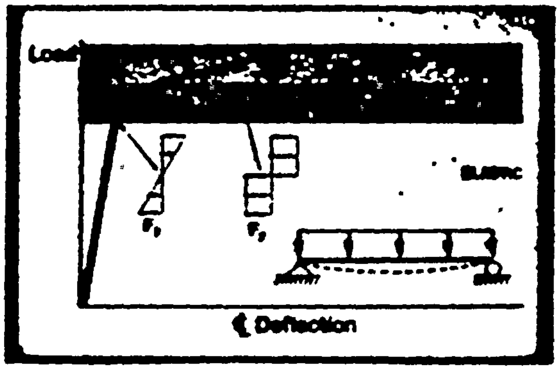

* Curves 1 and 2 treated together because the design provisions are basically the same.

* Local buckling and lateral buckling are controlled until significant yielding takes place.

* ASD - called compact sections.
  PD - when plastic design approaches are desired, this type of behavior must be assured.

* 1 is the most common structural situation. Load increases due to a moment gradient and strain hardening - moment varies along the length. Strain hardening strength is neglected in design 2 for a uniform moment region and is also an idealization of 1.

Slide No. 2-10

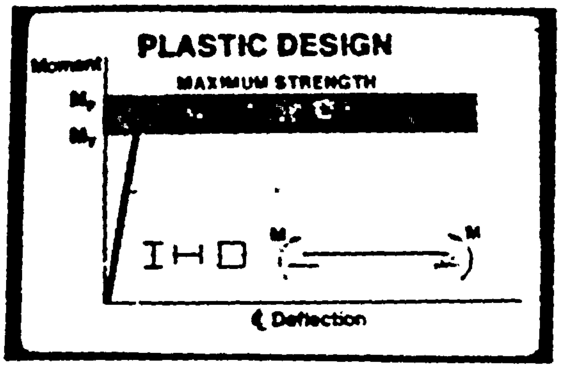

* Bending strength based on full yield of cross section. Takes full use of each type of section.

* Load factor = 1.7 for gravity loads regardless of type of cross section.

* Not concerned with some slight local yielding at working load because yielding will always occur due to residual stress, stress concentration, erection, etc. Also, once one cycle of loading and unloading occurs, further response is elastic.

* Maximum strength without strain hardening.

Slide No. 2-11

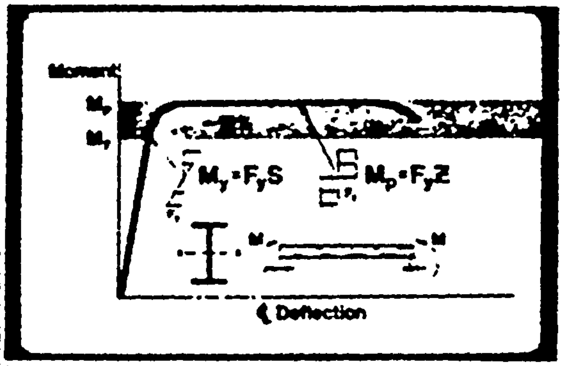

* H-Shape bent about x-x axis. Spacing of lateral bracing and width-thickness ratios of flange and web small enough to avoid local buckling until the entire cross section has yielded.

* On the average, plastic strength about 12% higher than 1st yield for H-shape sections.

Slide No. 2-12

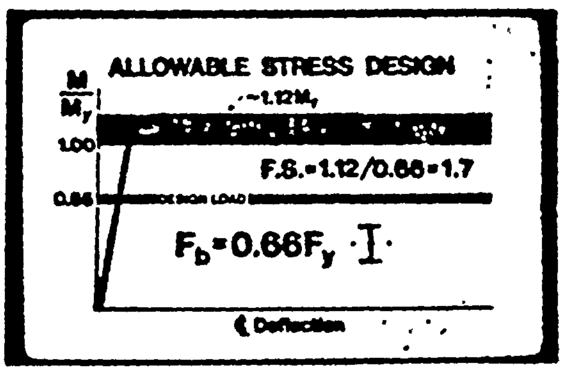

* Basing the factor of safety on full yielding of the cross section, not first yield, F.S. = 1.7.

* Actual design differs from plastic design in that only limited inelastic deformation is counted on.

* However, almost all provisions (compact sections) in ASD are based on this higher strength.

Slide No. 2-13

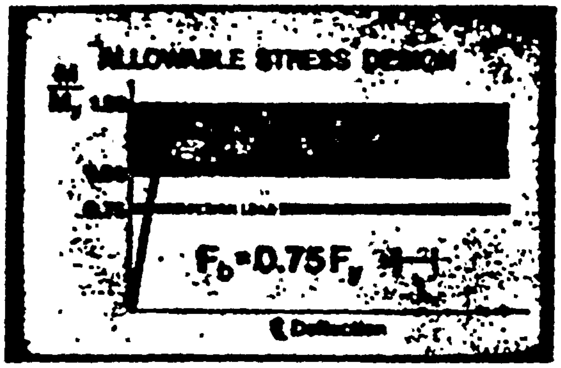

* Allowable bending stress is increased to 0.75 F_y when bending occurs about the weak axis because of large reserve strength beyond first yield (50% here).

* Still has more than adequate F. S. = 2.0.

* Margin of safety is provided against yielding at work load.

* Use $.75F_y$ for sections with good reserve strength like solid sections.

* Do not use for box or tubular members.

Slide No. 2-14

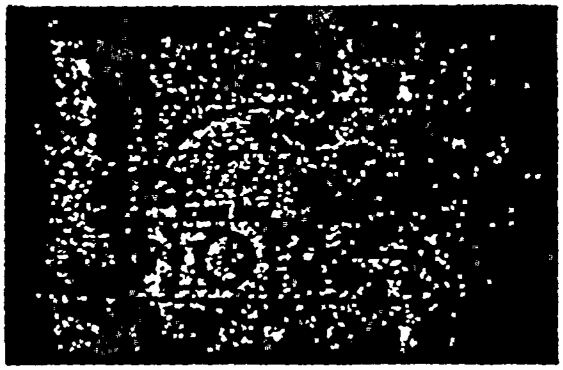

* Round sections subjected to bending reach their ultimate capacity in one of three basic failure modes;

   1. For very thick sections the compressive capacity of the material is reached, which means that large distortion occurs with no drop-off in the load.

   2. Thinner round sections fail by excessive ovalization of the cross section. This is a type of inelastic instability problem in which the decrease in moment capacity caused by the reduction in the section modulus due to flattening occurs more rapidly than the increase in moment.

   3. Very thin cylinders fail in a diamond shaped local buckling pattern.

* The division between ovalization and local buckling is taken as $3300/F_y$ which is the D/t limit given in the AISC Specification for compact circular sections.

* Ovalization will not impair the development of the plastic hinge in tubes with D/t less than $1300/F_y$. See Sherman, D. R., "Tentative Criteria for Structural Applications of Steel Tubing and Pipe", AISI, Washington, D.C. 1976

Slide No..2-15

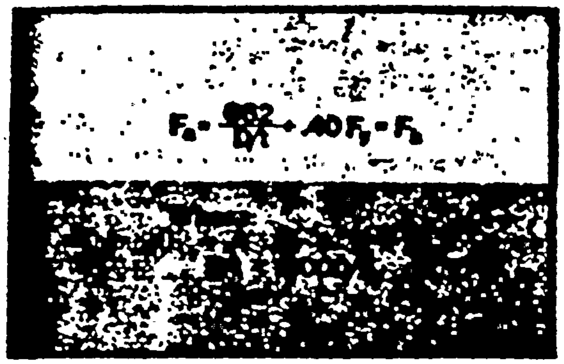

* What the allowable bending stress is for circular sections that exceed the D/t = 3300/F_y limit?

* Appendix "C" of the AISC Spec. gives this formula for allowable axial stress when tubular members do not meet the D/t requirements necessary for stiffened elements subject to axial compression.

* This same formula is applicable to an allowable bending stress as long as the D/t ratio does not exceed 13,000/F_y.

NOTE:
See page 5-95 of Appendix C for background. Also, Page 9 of "Tentative Criteria for Structural Applications of Steel Tubing and Pipe", D. R. Sherman, AISI Publication.

Slide No. 2-16

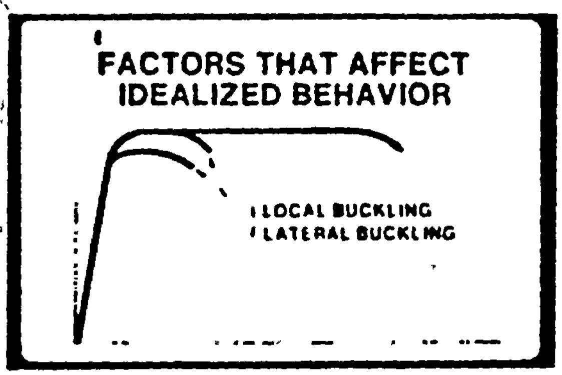

* The two previous solutions are based on the idealized behavior (shown solid).

* To achieve this behavior, lateral buckling and local flange and web buckling must be controlled.

* One or both will always eventually cause failure of the member, but only after the structure becomes useless because of excessive deflection.

* Sections that satisfy the width-thickness and bracing requirements are called compact sections.

Slide No. 2-17

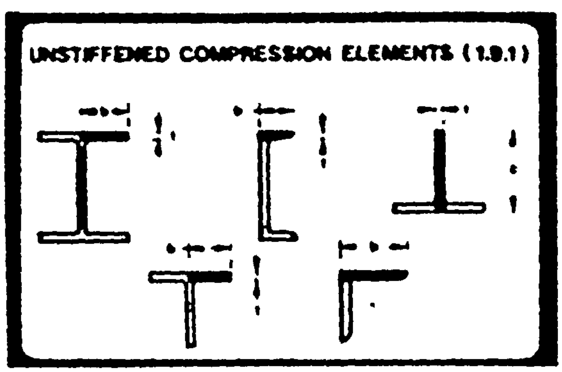

* Width-thickness ratios are defined in Spec. Section 1.9.1.

* Thickness is average for elements like flanges of channels and "I" (S Shapes).

* Appendix C used when values in Section 1.9.1 are exceeded.

Slide No. 2-18

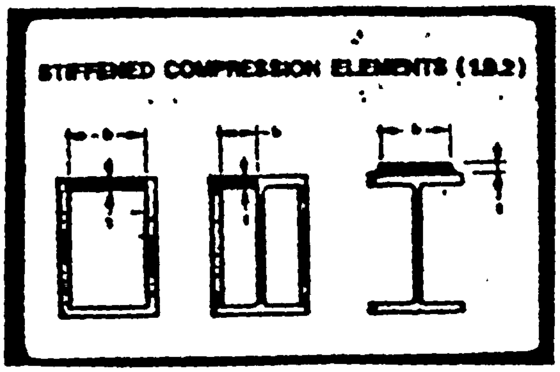

* Stiffened compression elements are also defined in Section 1.9.2 of Specs.

* Sections shown can be compact.

Slide No. 2-19

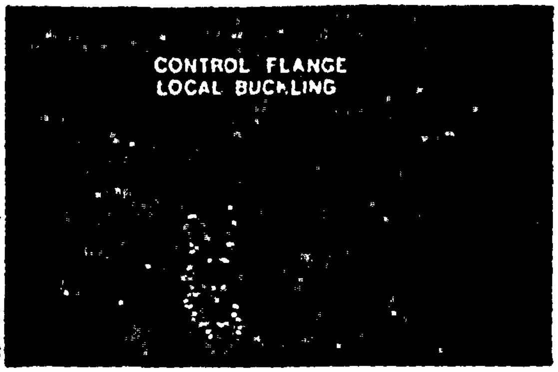

* Relationship between width-thickness ratio of unstiffened compression flanges and yield stress.

* Give values for A36 steel. 21.6 for ASD/LRFD and 17 for PD.

* The differences in ASD and PD requirements is that PD may require large rotation capacity - thus local buckling more critical.

* ASD requirements are based on a compact section that assumes an inelastic rotation capacity of 3. When a higher rotation capacity is required, then the b/t requirements would be tightened to those of plastic design.

* Experimental data are limited for the very high strength steels, so use of compact behavior and plastic design only for steels up to F_y = 65 ksi.

* Combinations of F_y and b/t that fall in the shaded area satisfy the AISC compactness requirements.

Slide No. 2-20

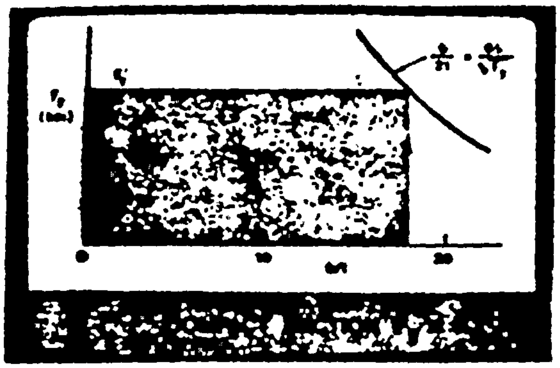

* For a given b/t, the yield stress which just satisfies the equation can be calculated. It is called F_y'.

* For each rolled section, the b/t is known so F_y' can be determined. If the yield stress is greater, you do not satisfy the equation and cannot use $0.66\ F_y$. If the yield stress is less than F_y', the cross section satisfies the requirements for a compact section to control local flange buckling.

* Values of F_y' are tabulated in the AISC Manual for rolled sections under the PROPERTIES FOR DESIGNING.

Slide No. 2-21

* Web slenderness requirements for compact sections try to ensure web yielding before web buckling starts.

* Web buckling depends on the stress distribution in the web; the presence of axial force in addition to the moment alters the stress in the web, so compact section criteria for webs includes effect of axial stress.

Slide No. 2-22

* If axial load is zero, $d/t = 640/\sqrt{F_y}$. Half of the web is in tension, the other half is in compression.

* When $f_a/F_y \geq 0.16$, entire web will have a uniform compressive stress distribution at ultimate load.

* Give values of d/t limits for A36 steel.

  - No axial load, $d/t \leq 107$
  - $f_a/F_y \geq 0.16$, $d/t \leq 43$

* The formula shown is for ASD, and is also applicable to PD when no axial load is present. An inelastic rotation capability of 3 is assured. For a greater rotation capacity, d/t is limited to $412/\sqrt{F_y}$ in PD.

Slide No. 2-23

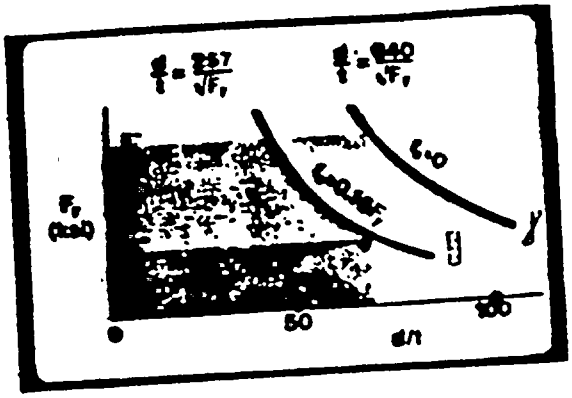

* If no axial load is present $F_y \leq F_y''$, the web is compact.

* F_y'' is the hypothetical yield stress above which the section is non- compact due to web criteria.

* When axial load is present and $F_y < F_y'''$, the web is compact. If F_y is between F_y''' and F_y'', check the formula for d/t requirements.

* Actually, all shapes now available conform to $d/t \leq 640/\sqrt{F_y}$ with available steels. Therefore F_y'' is not required.

Slide No. 2-24

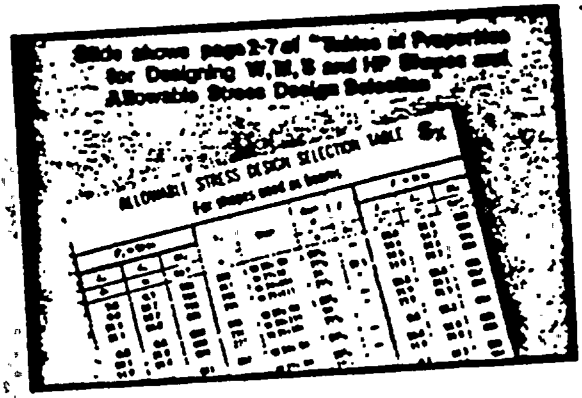

* Slide shows page 32 of "Tables of Properties for Designing W.M.S. and HP Shapes and Allowable Stress Design Selection.

Slide No. 2-25

* Lateral buckling affected by:

  - Steel strength.
  - Unbraced length of compression flange.
  - Moment gradient.

* Bracing must be spaced close enough to prevent lateral buckling from significantly affecting the idealized behavior.

Slide No. 2-26

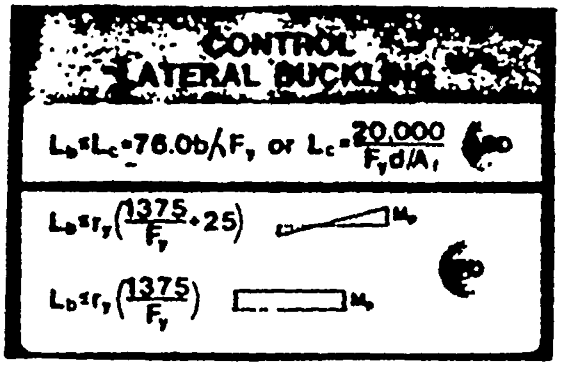

* Lateral buckling control is not completely understood to date as evidenced by the vast difference in appearance between the formulas for ASD and PD.

* ASD Formulas involve four different cross sectional properties, and the checking of two formulas.

* Governing L_c listed in AISC Manual in Beam Load Tables for beam-type cross sections.

* Formulas are based on thorough tests.

* Uniform Moment if $-0.5 > M/M_p > 1.0$.

* ASD makes no distinction between uniform moment and moment gradient but PD.

Slide No. 2-27

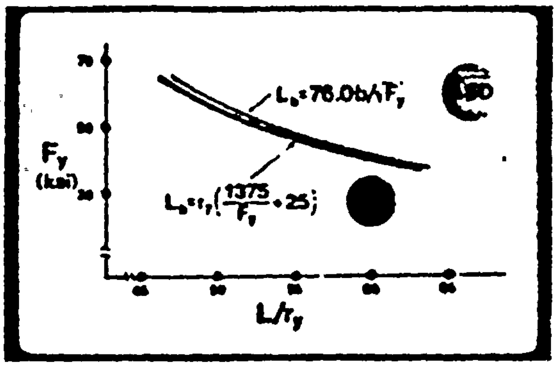

* ASD/PD provisions shown are almost identical.

* PD curve is for moment gradient case.

* Only for the case of uniform moment will plastic design require L_c, ASD may require a shorter bracing spacing than that for ASD.

* Since ASD requires checking another formula which <u>could</u> govern L_c, ASD may require a closer bracing spacing than PD.

* Safe region is below curves.

Slide No. 2-28

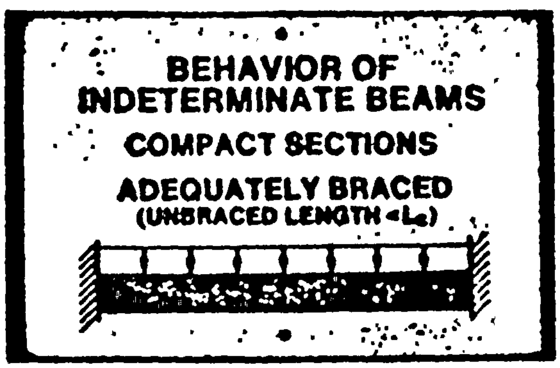

* ASD - limit of usefulness is based on yielding of the cross section at one point only.

* PD - limit of usefulness = ultimate load.
  - apply load factor to working load. (1.7)

Slide No. 2-29

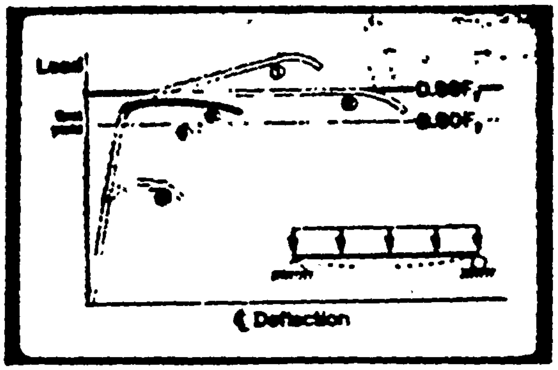

* Behavior illustrated by curve (3) should be expected if lateral buckling is controlled but flange or web slenderness ratios exceed compactness limits.

* PD not permitted. No moment redistribution permitted.

* ASD permits gradual change in allowable stress between $.6F_y < F_b < .66F_y$ when flange compactness limits are exceeded.

* Historically the AISC Spec. does not permit local buckling below 1st yield in hot rolled members.

Slide No. 2-30

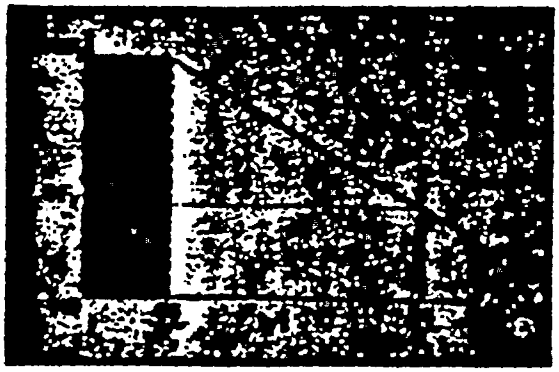

* Shows local buckling criteria in AISC Spec.

* $F_b = 0.66\ F_y$ for b/t up to $65/\sqrt{F_y}$.

* Straight line transition to $F_b = 0.6F_y$ at b/t $= 95/\sqrt{F_y}$.

* Appendix C for b/t > $95\ \sqrt{F_y}$.

* Here, b is the width of the unstiffened element.

Slide No. 2-31

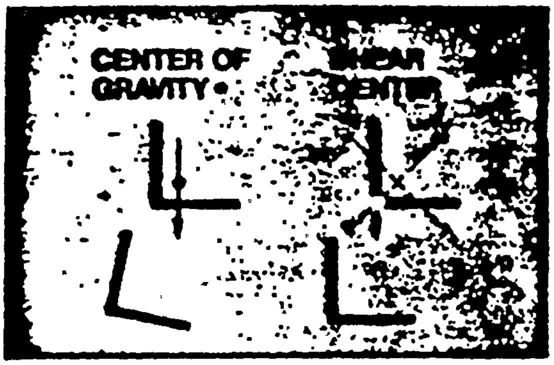

* Now is a good time to discuss the angle which is a very common member in building construction, but has limited design guidance available to the engineer.

* What design criteria that is available consists mainly of empirical extrapolations of solutions for other shapes and continued misconceptions about non-principal axis loading and shear center eccentricities.

* The design condition which presents the designer with a major information gap occurs when the angle is used as a laterally unsupported beam.

* The angle is a difficult shape for stress analysis.

* The principal axes of the cross-section do not coincide with common loading directions and any routine loading will therefore cause biaxial bending deflections which are not in the same plane as the applied loads.

* To further complicate the problem, the shear center is not at the centroid and is not on the line of most major applied loads. Thus most loads will cause the cross-section to twist and to deflect out of its loading plane.

* Finally, commonly used end connections are usually eccentric because of the lack of symmetry of the cross-section.

Slide No. 2-32

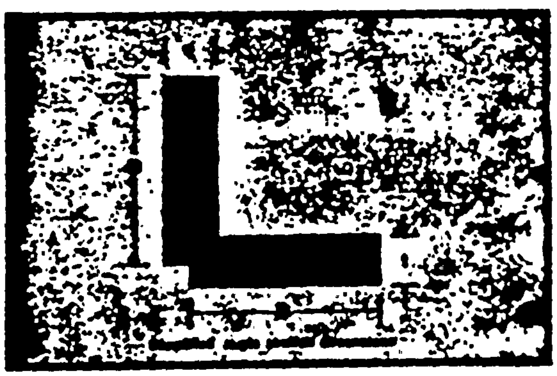

* There was a study made in Australia which developed some rational, simple formulas for the design of laterally unsupported angles in bending. See hand-out material.

* The theoretical study had these parameters:

  1. The loading resulted in uniform moment along the entire laterally unsupported span, which will produce the most critical lateral buckling situation.

  2. The angle lengths were assumed to be completely laterally unsupported.

  3. The following slides are applicable to equal leg angles, although similar research results on unequal leg angles are available. See hand-out material.

  4. The sections are approximated by the dual rectangle idealization shown. This linearized section ignores fillets and toe radii, but can be made to reproduce actual member properties very precisely by adjusting the idealized leg length, B, to produce an exact similitude for some chosen geometrical property (such as area). The assumption, therefore, is not critical and is necessary in order to obtain a solvable set

Slide No. 2-33

* The following slides will show how practical angle sections are usually governed by stress ($F_b = 0.6F_y$) or be deflection limitations rather than buckling.

* Case I is a common design situation, so let's briefly examine the Australian work for this case.

* Loading is as shown with M_a being the applied moment, which is resolved into components about the major principal axis U, and the minor principal axis V.

* If the maximum stress were calculated without resolving the applied load into U and V components, the result could be unconservative by as much as 50%.

Slide No. 2-34

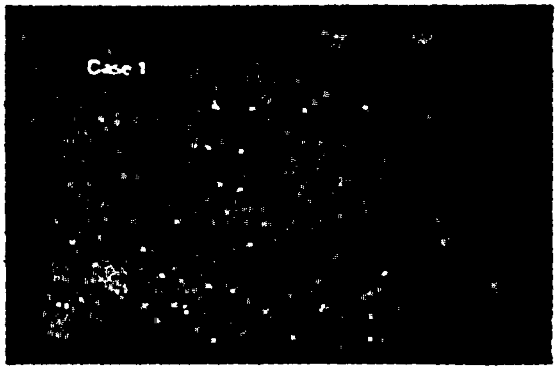

* The Australian study showed that for laterally unrestrained angle beams the following relationships apply:

* The stress at any point in the section is

$$\frac{3M}{b^3 t} [(V + 4U) \phi_1 + V - 4U]$$

where V and U are cordinate points normal to the principal axes.

* Max. Section Stress is as shown.

* Angle of twist ϕ_1 is made up of ;
ϕ = twist due to applied loads
ϕ_e = initial angle of twist due to imperfections.

Slide No. 2-35

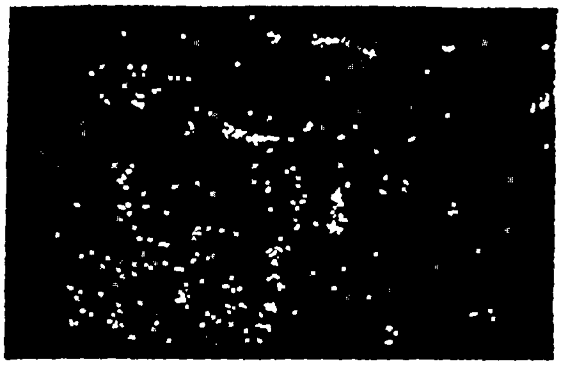

* The top equation shows that the stress in the section is a linear function of the amount of twisting (ϕ) to which it has been subjected.

* ϕ also has a direct relation to

$L/_t$, $\frac{\sigma_a}{E}$ and $\frac{B}{t}$

Where: $\sigma_a = \frac{M_a}{Z_a}$ does not include stress due to twist.

Z_a is elastic section modulus (Australian nomenclature).

Slide No. 2-36

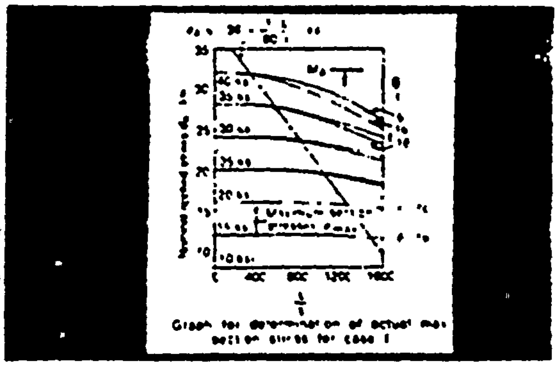

* Thus it is possible to produce curves of σ_a against L/t with contours of σ_{max}, the maximum section stress.

* Twisting may be ignored if,

$$\sigma_a \leq (38 - \frac{1}{60} \times \frac{L}{t})\ \text{ksi}$$

* Later research on unequal leg angles confirms, in general, $\sigma_{max} = 1.25\ \sigma_a$.

Slide No. 2-37

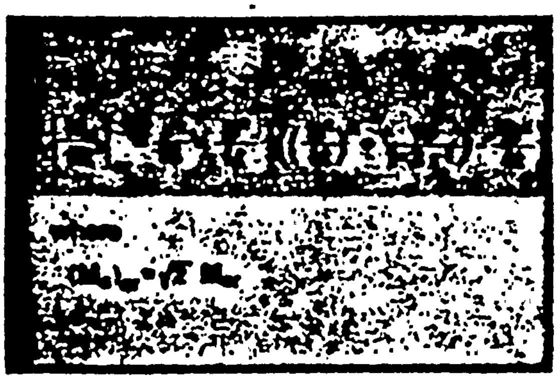

* An alternative method of angle beam design for Case I is to consider the critical buckling moment given by this formula .... where the critical applied moment is equal to $\sqrt{2}$ times the critical buckling moment.

* The dimensionless parameters $\frac{M_a}{Et^3}$ & $\frac{B^2}{Lt}$ are then used to draw the critical buckling curve.

Slide No. 2-38

* This curve allows the estimation of the critical applied moment for a given length and section.

* The horizontal lines represent the values of $\frac{M_a}{Et^3}$ necessary to produce a stress of $3F_y$, for various $\frac{B}{t}$ ratios.

* It was shown that failure stresses will be unaffected by elastic buckling if the calculated buckling stress is at least three times the material yield stress.

* Shaded area shows design range. For instance, with B/t of 16 and a stress of 3Fy, $\left[\frac{L}{t}\right]\cdot\left[\frac{t}{B}\right]^2 = 2.7$.

  Therefore, $\frac{L}{t} = (16)^2 \times 2.7 = 690$. Similar calculations for other B/t ratios can be made.

Slide No. 2-39

Case	B/t	Range for $F_b = 0.66\,F_y$
F=36 ksi	6	$0 < L/t < 990$
	11	$0 < L/t < 850$
	16	$0 < L/t < 690$

* Therefore, Australian research indicates that allowable bending stress F_b may be taken as $0.66\ F_y$ for these limitations on $B/_t$ and $L/_t$.

* It has been practice in U.S. to use $F_b = 0.6F_y$.

* At these high stresses, deflection may control.

Slide No. 2-40

* The critical stress corresponding to the critical applied moment can be obtained (upper equation), and then converted into a safe bending stress (F_{bc}) thru use of these two formulas from the Australian Steel Structures Code AS CA 1.

* Again, shaded area represents design range. As before $\left[\frac{L}{t}\right]\cdot\left[\frac{t}{B}\right]^2$ can be seen as approximately 2.7.

Slide No. 2-41

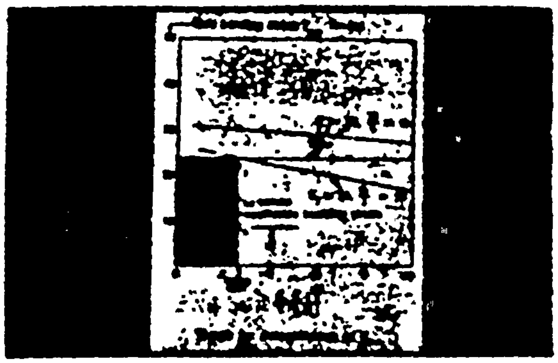

* The result of converting the critical stress into a safe bending stress is shown here in graphic form, which may be used directly for design.

* A copy of the Australian research report is enclosed within the handout you received. Hopefully it will assist you when designing angle beams in the future.

Slide No. 2-42

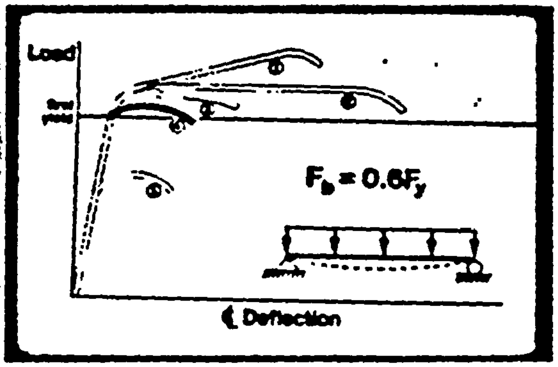

* Curve 4 is typical of sections with non-compact webs - welded girders in general.

* Also typical of box girders that are unbraced laterally.

* $F_b = 0.6\ F_y$.

* Curve 5 is typical of beams which fail by local or Lateral Torsional Buckling (LTB) and will be covered in a later lecture.

Slide No. 2-43

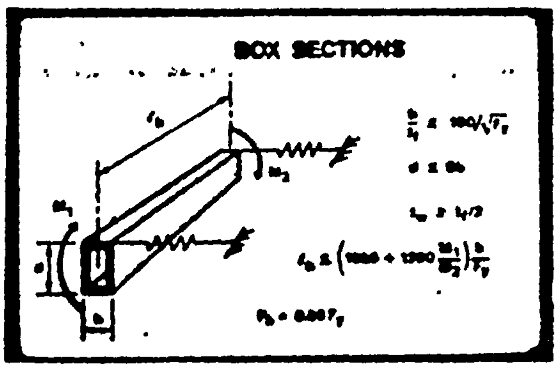

* Box sections may be compact.
  Also less susceptible than W-shapes to lateral torsional buckling.

* Criteria for compactness shown

  b/t less than $190/\sqrt{F_y}$
  $d \leq 6b$ and $t_w \geq t_f/2$

* Also a bracing requirement which takes into account moment gradient. Moments shown are in plane of beam.

* M_1/M_2 same as defined in other part of Spec.

* L_b need not be less than $1200(b/F_y)$.

Slide No. 2-44

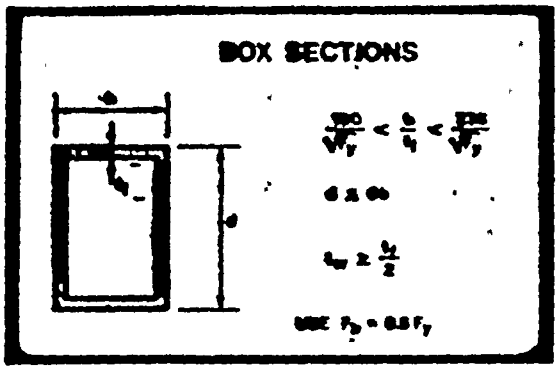

* If box sections do not meet compactness requirements use $F_b = 0.6\ F_y$.

* No lateral torsional buckling consideration if d less than 6b, and $t_w \geq t_f/2$.

* Unbraced length does not affect carrying capacity. Deflection will govern with very long spans.

Slide No. 2-45

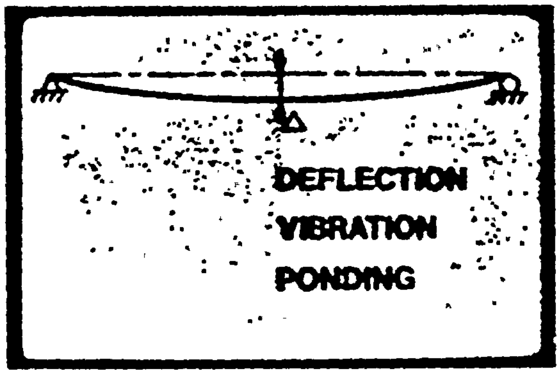

* The design of beams in a floor or roof system would not be complete without some attention to Deflection, Vibration and Ponding. Sometimes these are criteria for design rather than stres. .

* While the Specification does require that Deflection, Vibration and Ponding be considered the only precise limits enumerated are the 1/360 of the span live load deflection for beams supporting plaster ceilings and the Ponding Formulas to be checked for flat roofs. We will look at the ponding formulas in detail later.

* Deflection limits must rest on the sound judgment of the designer and the experience of the behavior of similar structures. The Commentary to the AISC Specification gives as a guide the following:

  Fully stressed floor beams and girders; F_y depth not less than $F_y/800$ times the span.

  Fully stressed roof purlins (except in flat roofs) depth not less than $F_y/1000$ times the span.

  For A36 steel these recommendations work out to be approximately 1/22 for floor beams and 1/28 for the roof purlins.

* Large open floor areas free of partitions or other sources of damping may be susceptible to transient vibration due to pedestrian traffic. While there are some design methods available to check a floor system for vibration susceptibility they necessarily involve trying to evaluate the difficult problem of human perception of vibration. The Commentary recommends as a guide the depth of a steel beam be not less than 1/20 of the span where a problem of perceptible transient vibration might be suspected.

Slide No. 2-46

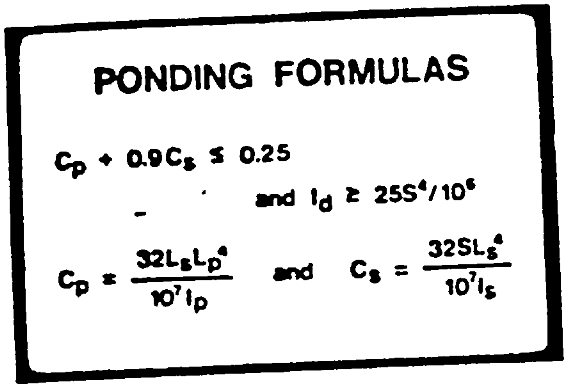

* Spec. Sect. 1.13 gives approximate but conservative formulas for ponding.

* Point out the more exact method in the Commentary.

* C_p and C_s are ponding coefficients.

Slide No. 2-47

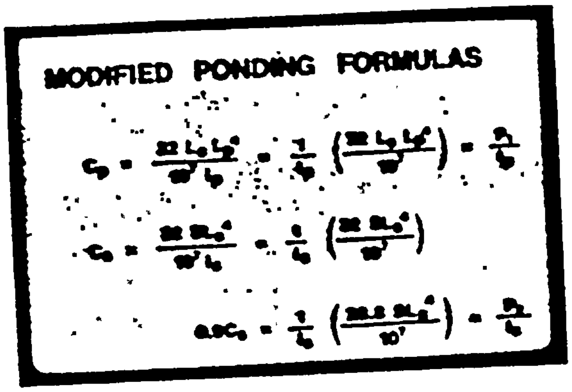

* Discuss the Modified Ponding Formulas. Show how they were derived.

  (AISC Engineering Journal - First Quarter, 1973, Page 26)

* Modified Ponding Formulas derived by Burgett, "Fast Check for Ponding", Eng. Journal, 1st Quarter, 1973.

Slide No. 2-48

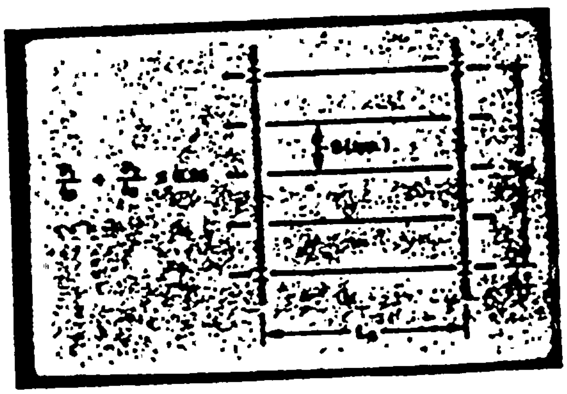

* Definition of symbols shown on typical roof framing plan.

Slide No. 2-49

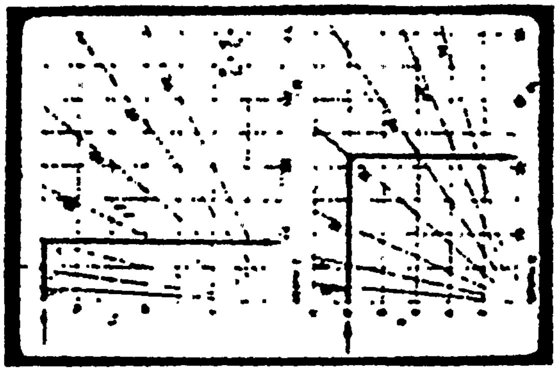

* Graphs I and II have been developed to determine P_1 and P_2 which are available in Burgett paper.

Slide No. 2-50

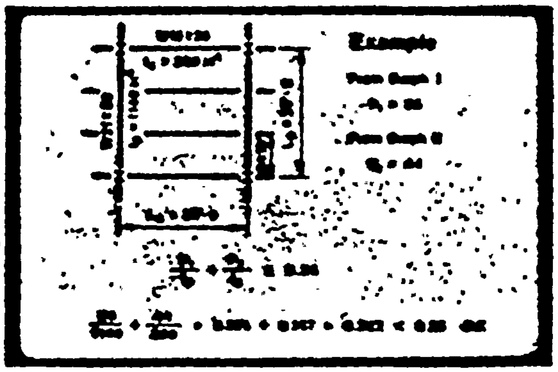

* Design Example

* Illustrates the use of Graphs I and II.

Slide No. 2-51

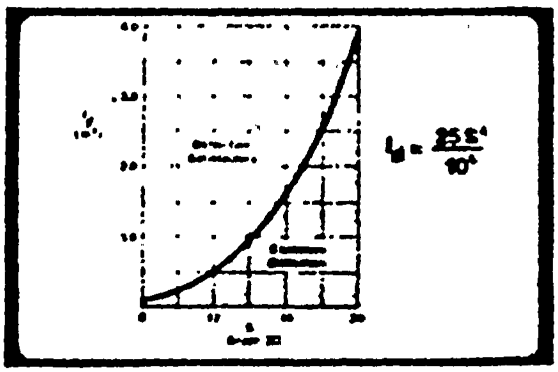

* Illustrates the use of graph III and the check for steel deck.

The design of laterally unsupported angles

J. M. Leigh
Experimental Officer
Melbourne Research Laboratories
M. G. Lay
Principal Research Officer
Melbourne Research Laboratories

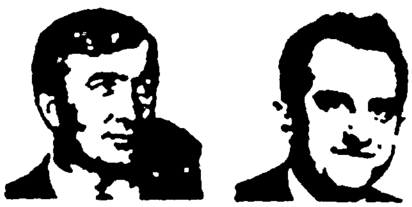

1. Introduction

The steel angle is a common and almost traditional member in building construction. Its popularity stems from its relative lightness and compactness and the ease with which it can be connected to other members. In view of its long and widespread use it is surprising to find that little is known of many major aspects of its performance as a structural member. In these areas design guidance is only available to a limited extent and consists mainly of empirical extrapolations of solutions for other sections[1] and continued misconceptions about non-principal axis loading and shear centre eccentricities.

The behaviour of angles as compression members has been studied relatively extensively (e.g. [2, 3, 4]) as a result of their widespread use in such structures as transmission towers. These towers are usually precisely analysed[3] for actual failure under well defined load factors and an accurate knowledge of member load capacity has been essential. Even here, however, the underlying research has frequently been highly empirical with strut load capacities given for each member size under practical field conditions[6].

The case which presents the designer with his current major information gap occurs when the angle is used as a laterally unsupported beam. For example, the S.A.A. Steel Structures Code AS CA1[7] states in Rule 5.4.3:

> 'The Standards Association of Australia is not prepared at this stage to make recommendations for angles which are not supported laterally.'

The British Code permits its standard beam rules to be used for angles, but the technique developed can not be rationally defended[8, 9] and does not lead to consistent design solutions. The U.S. steel design specification[10] does not specifically cover the case.

The logical question to ask at this stage is why the problem of the laterally unsupported angle used as a beam has remained without a practical solution for so long. The answer is, basically, that although the angle is a very simple section to the layman and the producer, it is a difficult one for the stress analyst. The principal axes of the cross-section do not coincide with common loading directions and any routine loading will therefore cause biaxial bending deflections which are not in the same plane as the applied loads. To further complicate the problem, the shear centre is not at the centroid and is not on the line of most major applied loads. Thus most loads will cause the cross-section to twist and to deflect out of its loading plane. Finally, common end connections are usually eccentric because of the lack of symmetry of the cross-section.

2. Current Investigations

The purpose of the current investigation is to develop rational but simple formulas for the design of laterally unsupported angles in bending. This should help fill the present, previously quoted, void in the S.A.A. Steel Structures Code, CA1, and thus permit the more widespread use of angles in building construction.

The loading case to be considered will be a uniform moment along the entire laterally unsupported span. This will produce the most critical lateral buckling situation[11] and will therefore give results which will be safe for any other bending moment distribution. The same uniform moment basis is used for the other lateral buckling rules of CA1[12, 13]. The lengths under consideration are assumed to be completely unsupported and the solutions may therefore be applied to both fully unsupported beams or restrained beams between restraint points.

Later work will include an experimental examination of various aspects of the problem. However, this article will be confined to a theoretical derivation of design rules.

Solutions are only presented for equal angles (leg lengths equal). Similar solutions can be obtained for unequal angles, but the complete asymmetry of these latter sections produces algebraically involved results which tend to obscure the basic underlying principles.

The range of equal angles produced by BHP are given in [14]. The sections are approximated by the dual rectangle idealisation shown in Fig.1. This linearised section ignores fillets and toe radii, but can be made to reproduce actual member properties very precisely by adjusting the idealised leg length, B, to produce an exact similitude for some chosen geometrical property (such as area). The assumption, therefore, is not critical and is necessary in order to obtain a solvable set of equations.

3. Notation and sign convention

The notation to be used is:

B = Width of angle leg.
A, C, D = Constants of integration.
E = Young's Modulus.
F = Design stress.
F_c = Critical buckling stress.
F_b = Maximum permissible bending stress.
F_y = Yield stress.
G = Modulus of rigidity (shear or torsion modulus)
I_U = Second moment of areas about UU axis.
I_V = Second moment of area about VV axis.
I_W = Warping moment of area.
K_T = St. Venant torsional constant.
$\overline{K}$ = Torsional component of the normal stress (see eq.5.4).
L = Length of span.
M = Component moment of the applied moment.
M_{cr} = Critical buckling moment.
M_a = Applied moment about Y axis + moment due to the dead weight of the beam.
S = Shear centre.
U Denotes the major principal axis.
V Denotes the minor principal axis.
W Denotes the polar axis.
Y, X Denotes axes through the centroid, parallel to an angle leg.
Z = Section modulus.
Z_a = Section modulus about same axis as M_a.
Z_v = Section modulus through the V axis.
c = Centroid location.
t = Thickness of angle leg.
u = U—U axis co-ordinate.
v = V—V axis co-ordinate.
u_o = Shear centre co-ordinate.
v_o = Shear centre co-ordinate.

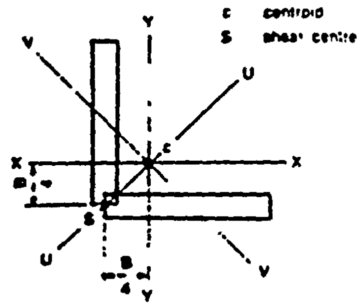

Fig 1 (a). Orientation of axes and locations of centroid and shear centre.

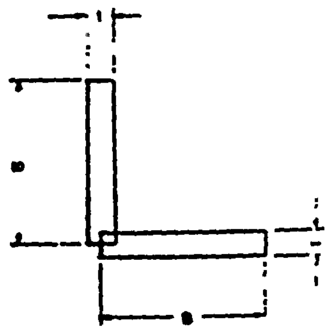

Fig.1 (b). Simplified angle section dimensions

w = Distance measured along the length of the beam.
σ = Actual section stress.
σ_s = Stress calculated using conventional beam formula:

$$\sigma_s = \frac{M_s}{Z_s}$$

σ_{cr} = Critical buckling stress.
ϕ = Angle of twist.
ϕ_o = Initial angle of twist due to imperfections.
α = Coefficient in solution of differential equations.
$'$ = Differentiation with respect to w.

This notation is coupled with the sign convention shown in Fig.2.

4. Loading cases

The behaviour of the beam is dependent on the axis about which the moment is applied, Fig.2. Four loading conditions are illustrated in Fig.3. These conditions can be used vectorially to represent all possible cross-section loadings. Taken individually they are:

Case I: Moment applied about an axis through the shear centre parallel to one leg.

Case II: Moment applied about the UU axis (strong axis).

Case III: Moment applied about the VV axis (weak axis).

Case IV: Moment applied about an axis midway between the UU axis and the YY axis.

Each of these cases will now be individually studied.

5. Case I

The problem to be solved is illustrated in Fig.3(a) and Fig.4. Galambos[15] has shown that for this case the following equations apply*:

Bending in the V Direction:

$$\text{(3.81)}\quad EI_T v'' + M\phi = -M \qquad \text{—(5.1)}$$

Bending in the U Direction:

$$\text{(3.82)}\quad EI_t u'' + M\phi = M \qquad \text{—(5.2)}$$

Torsional Equilibrium:

$$\text{(3.83)}\quad EI_\omega \phi''' - (GK_T + \bar{K})\phi' + Mu' + Mv' = 0 \qquad \text{—(5.3)}$$

where the symbols are as defined in Section 3 and the primes indicate differentiation with respect to w, the distance along the beam.

The equations are derived from the following set of assumptions:

(a) The material is elastic.
(b) The member is straight and prismatic.
(c) The cross-section is thin walled and open.
(d) Deflections are small.

All the constants are readily calculable (see Sect.4) with the exception of I_ω and $\bar{K}$. It has been shown in [18] that warping is insignificant for angle sections, therefore, $I_\omega = 0$. $\bar{K}$ can be determined from the following constitutive equations given by Galambos:

$$\text{(3.86)}\quad \bar{K} = M(\beta_u - \beta_v) \qquad \text{—(5.4)}$$

$$\text{(3.13)}\quad \beta_u = \frac{1}{I_u}\int_A v(v^2 + u^2)t\,ds - 2v_o \qquad \text{—(5.5)}$$

$$\text{(3.86)}\quad \beta_v = \frac{1}{I_v}\int_A u(u^2 + v^2)t\,ds - 2u_o \qquad \text{—(5.6)}$$

*The left hand equation numbers correspond to those in Galambos[15].

For the idealised section (Fig.1)

$$v = \pm\left(u + \frac{B}{2\sqrt{2}}\right)$$

and $ds = \pm\sqrt{2}du = \sqrt{2}dv$

Integration of equations (5.5) and (5.6) yields

$\beta_u = 0$ and $\beta_v = \sqrt{2}B$

whereupon:

$$\bar{K} = -\sqrt{2}BM \qquad \text{—(5.7)}$$

for equal angle sections.

The angle of twist ϕ may now be determined by substituting this solution into eq. (5.3) to give:

$$-(GK_T - \sqrt{2}BM)\phi' + Mu' + Mv' = 0 \quad (5.8)$$

Differentiating this and substituting values of u'', v'' from (5.1), (5.2) gives:

$$\lambda_1\phi'' + \lambda_2\phi = -\lambda_3 \qquad \text{—(5.9)}$$

$$\lambda_1 = GK_T - \sqrt{2}MB \qquad \text{—(510)}$$

$$\lambda_2 = \frac{M^2}{E}\left(\frac{1}{I_v} + \frac{1}{I_u}\right) \qquad \text{—(5.11)}$$

$$\lambda_3 = -\frac{M^2}{E}\left(\frac{1}{I_v} - \frac{1}{I_u}\right) \qquad \text{—(5.12)}$$

The general solution is:—

$$\phi = A\cos\alpha w + D\sin\alpha w - \frac{\lambda_3}{\lambda_2} \qquad \text{—(5.13)}$$

where $\alpha = \left(\frac{\lambda_2}{\lambda_1}\right)^{1/2}$

with boundary conditions:

$$\phi_{(w=0)} = \phi_{(w=L)} = 0$$

one obtains

$$\phi_{max} = \frac{3}{5}\left(1 - \frac{1}{\cos\alpha L/2}\right) \qquad \text{—(5.14)}$$

6. Case I. Critical buckling

For Case I the critical buckling condition occurs when:

$$\alpha L = \pi$$

as at this value

$$\phi = -\infty \text{ (see eq. 5.14).}$$

Since

$$\alpha L = \left(\frac{\lambda_2}{\lambda_1}\right)^{\frac{1}{2}} . L$$

the critical moment is given by:

$$\pi = \frac{7 \cdot 65ML}{B^2Et^2\left(1 - \frac{5 \cdot 5M}{Et^2}\right)^{\frac{1}{2}}} \qquad \text{—(6.1)}$$

or

$$\left[\frac{M_s}{Et^2}\right]_{cr} = \frac{\pi^2}{15} \cdot \frac{B^2}{Lt}\left[\left(\left(\frac{B^2}{Lt}\right)^2 + \frac{10}{1 \cdot 3\pi^2}\right)^{\frac{1}{2}} - \frac{B^2}{Lt}\right] \qquad \text{—(6.2)}$$

where

$(M_s)_{cr} = \sqrt{2}M_{cr}$ = the critical applied moment and the dimensionless parameters $\frac{M_s}{Et_s}$ and $\frac{Lt}{B^2}$ are used to draw the critical buckling curve (Fig.5a). This curve allows an estimation of the critical applied moment for a given length and section. The horizontal lines represent the values of $\frac{M_s}{Et^2}$ to produce a stress of $3F_y$ (where F_y is the material yield stress), for yield stresses of 52 and 36 ksi and $\frac{B}{t}$ ratios of 6 and 16.

It has been shown[18, 19] that failure stresses will be unaffected by elastic buckling if the buckling stress is at least three times the material yield stress.

Thus, it can be established that F_b may be taken as $0 \cdot 66\ F_y$ for the following cases:

Case	B/t	Range for $F_b = 0 \cdot 66\ F_y$
$F_y = 52$ ksi	6	$0 < L/t < 680$
	11	$0 < L/t < 570$
	16	$0 < L/t < 330$
$F_y = 36$ ksi	6	$0 < L/t < 990$
	11	$0 < L/t < 850$
	16	$0 < L/t < 690$

The critical stress corresponding to the critical moment in eq.6.2 can be obtained by:

$$\sigma_{cr} = \frac{(M_s)_{cr}}{Z} = \frac{9}{\sqrt{2}} \cdot \frac{(M_s)_{cr}}{B^2t}$$

$$\sigma_{cr} = 0 \cdot 424\pi^2\frac{Et}{L} \cdot \left[\left(\left(\frac{B^2}{Lt}\right)^2 + \frac{10}{1 \cdot 3\pi^2}\right)^{\frac{1}{2}} - \frac{B^2}{Lt}\right] \qquad \text{—(6.3)}$$

This stress corresponds to F_o in Rule 5.4.3 of AS CA1 and the safe bending stress F_{bc} for the beam can be calculated using eqs.(4) and (5) of those rules as the purpose of these equations is to permit such conversions to be made [12, 13]. The result of converting σ_{cr} in eq.(6.3) into F_{bc} is shown in Fig.5b, which may thus be used directly for design.

7. Case I. Stress solution

The actual maximum section stress is obtained from the stress equation, which gives the stress at any point in the section as:

$$\text{(2.74)}\quad \sigma = \frac{M_t v}{I_u} - \frac{M_v u}{I_v} + E\omega_n\phi'' \qquad \text{—(7.1)}$$

where $M_t = M(1 + \phi)$, $M_v = M(1 - \phi)$

It has been shown that the effect of warping is insignificant and since:

$$\text{(2.62)}\quad I_\omega = \int \omega_n^2 t\,ds = 0 \qquad \text{—(7.2)}$$

then $\omega_n = 0$

Equation (7.1) becomes:

$$\sigma = \frac{M(1 + \phi)v}{I_u} - \frac{M(1 - \phi)u}{I_v} \qquad \text{—(7.3)}$$

Substituting values for I_u, I_v gives:

$$\sigma = \frac{3M}{B^3t}\big((V + 4U)\phi + V - 4U\big) \qquad \text{—(7.4)}$$

This equation shows that the stress in the section is a linear function of the amount of twisting to which it has been subjected. The twist resulting from applied loads is given in eq.(5.14). Further twisting will result from initial eccentricities present in the unloaded angle. There are no specification limits for torsional eccentricity; however Massey[17] has measured the torsional eccentricity in steel I beams and suggests an average value of initial twist as:

$$\phi_o = 0 \cdot 436 \times 10^{-4}L \text{ radians} \qquad \text{—(7.5)}$$

Values measured for two angle lengths are given in Fig.7 together with Massey's general estimate. The method of measurement is shown in Fig.8. The twist due to the weight stress is avoided by measuring the total twist ($\phi_1 \cdot \phi_2$) of the angle in two positions ninety degrees apart. The measured values are in agreement with Massey's equation.

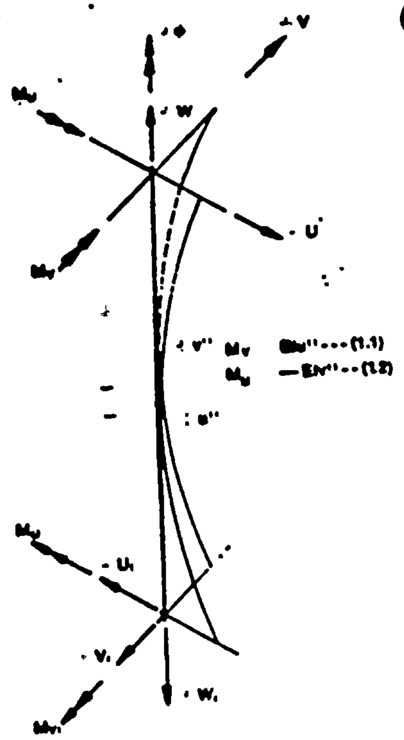

Note
Axes are drawn with W or W_1 as the outward drawn normal from the surface under consideration.

Fig.2. Sign convention

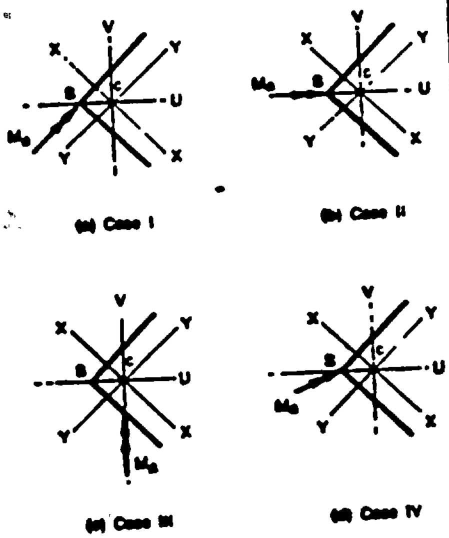

Fig.3. Loading for cases I to IV
(a) Case I
(b) Case II
(c) Case III
(d) Case IV

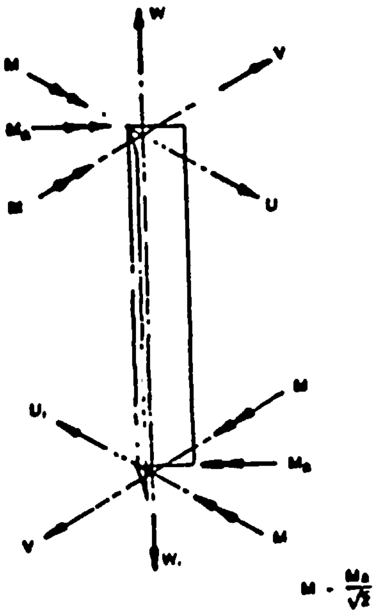

Fig.4 Loading for case I

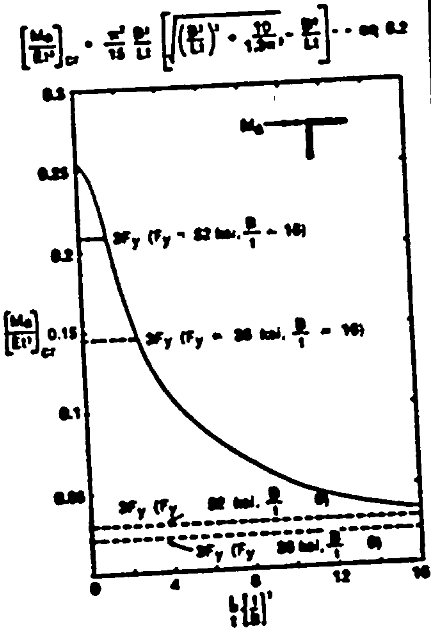

Fig.5 (a). Critical buckling curve for case I

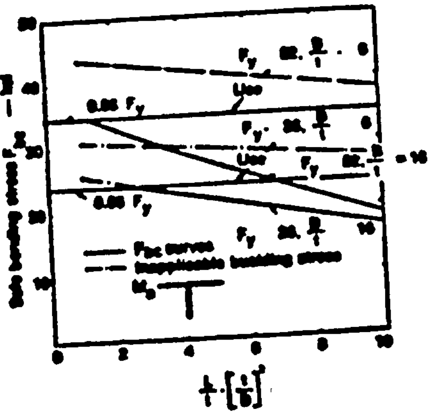

Fig.5 (b). Graph for determination of F_{bc} for case I

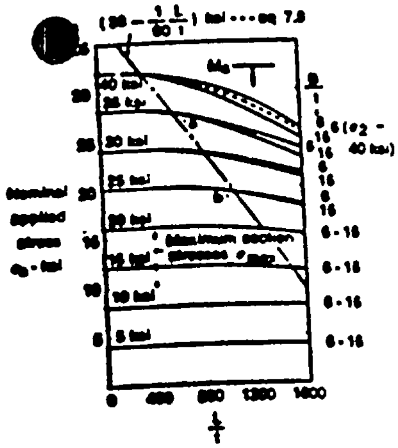

Fig.6. Graph for determination of actual max. section stress for case I

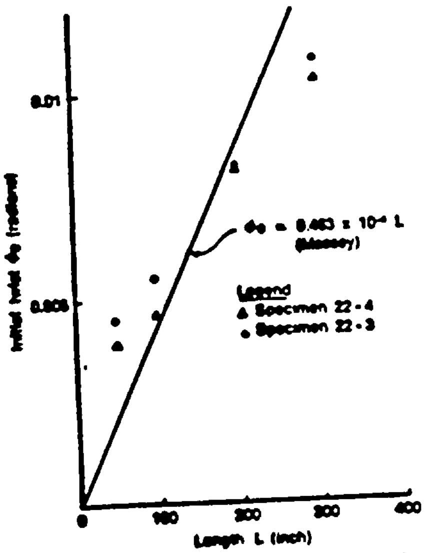

Fig.7. Initial twist ϕ_0 test results for angle sections compared with Massey's relationship

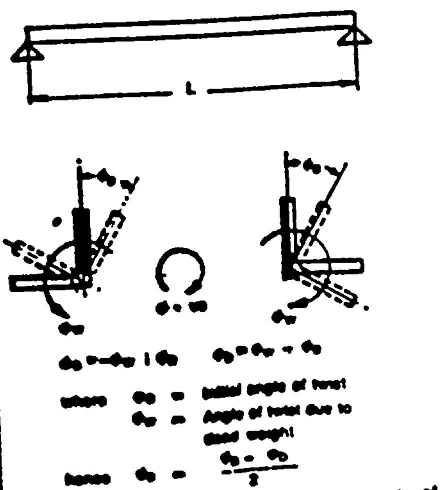

Fig.8 Method for determination of initial angle of twist

If ϕ_o is considered, the stress equation (7.4) becomes:

$$\sigma_o = \frac{3M}{B^2t}\left((V+4U)\phi_t + V - 4U\right) \quad —(7.6)$$

and if amplification effects near the buckling load are neglected

$$\phi_t = \phi + \phi_o = \frac{3}{5}\left(1 - \frac{1}{\cos \alpha L/2}\right)$$
$$+ 0{\cdot}436 \times 10^{-4}\left(\frac{L}{t}\right) \quad —(7.7)$$

where t in the ϕ_o part of the expression has been put equal to 1 to produce the maximum value of ϕ_o for values of $\left(\frac{L}{t}\right)$

It can be seen from Section 5 that

$\phi = f\left(\frac{L}{t}, \frac{\sigma_a}{E}, \frac{B}{t}\right)$,

where $\sigma_a = \frac{M_x}{Z_x}$ does not include the stress due to twist. Thus, it is possible to produce curves of σ_a against L/t with contours of σ_{max}, the maximum section stress, as shown in Fig.6. Contours of σ_t (stress including initial twist) are also shown. Although the initial twist does cause a stress increase over σ_{max} for the range examined; the magnitude of this increase is small and only apparent in the graph for large values of M and $(\frac{L}{t})$.

If the maximum section stress is calculated for Case I using conventional beam formulas and, if the applied moment is not resolved into components in the U and V axes, the calculated stress may be up to 50% less than the actual stress produced in the member. In terms of the symbols used above, σ_a may be up to 50% less than σ_{max}.

It is clear from the graph that twisting may be ignored if:

$$\sigma_a < \left(38 - \frac{1}{60} \cdot \frac{L}{t}\right) \text{ ksi} \quad —(7.8)$$

The expression is empirically determined from the form of the contours in Fig.6.

The two points 'a' and 'b' on Fig. 6 are obtained from the buckling solution given in Fig.5a, as the points where buckling does not influence the results. It is seen that the two approaches lead to similar results as 'a' and 'b' lie close to eq.(6.11). The buckling approach relies on the F_o—F_b conversion of eq.(4) and (5) of CA1, whereas the maximum stress approach is based on limiting the true peak stress to permissible values. The two solutions will therefore lead to similar but not identical results and the selection of a method will depend on the formulation of the problem.

8. Case II

Galambos[15] has shown that, for singly symmetric sections subject to the loading shown in Fig.3(b), the equations for lateral torsional buckling are:

$$(3.49) \quad EI_V u'' + M\phi'' = o \quad —(8.1)$$
$$(3.50) \quad EI_w\phi'''' - (GK_T + M\beta_c)\phi'' + Mu'' = o \quad —(8.2)$$

Since $\beta_c = o$ (Sect.5) and warping is insignificant then

$$\lambda_a\phi'''' + \lambda_b\phi'' = o \quad —(8.3)$$

where

$$\lambda_a = GK_T \quad —(8.4)$$
$$\lambda_b = \frac{M^2}{EI_V} \quad —(8.5)$$

The general solution is:

$$\phi'' = A \sin \alpha w + D \cos \alpha w \quad —(8.6)$$

where

$$\alpha = \left(\frac{\lambda_b}{\lambda_a}\right)^{\frac{1}{2}} \quad —(8.7)$$

Applying the end conditions of zero torsional restraining moment,

$$\phi''_{(w=0)} = \phi''_{(w=L)} = o$$

gives

$$D = o$$

and

$$\sin \alpha L = o$$

The lowest critical moment occurs when:

$$\alpha L = \pi$$

i.e.

$$\left(\frac{\lambda_b}{\lambda_a}\right)^{\frac{1}{2}} \cdot L = \pi$$

or

$$M_{cr} = \frac{\pi E}{6\sqrt{1{\cdot}3}} \cdot \frac{B^2t^2}{L} \quad —(8.8)$$

This result can also be obtained using the St. Venant buckling solution,

$$M_{cr} > \frac{\pi}{L}\left(EI_vGK_T\right)^{\frac{1}{2}} \quad —(8.9)$$

Substituting $M_{cr} = \sigma_{cr} . Z_x$ in eq.(8.1) gives:

$$\sigma_{cr} = \frac{\pi Et}{2\sqrt{2{\cdot}6}\ L} \quad —(8.10)$$

which is the critical elastic buckling stress for the member. Using the 'elastic critical stress to design stress' conversion of the SAA Steel Structures Code CA1, Rule 5.4.3, eqs.(4) and (5), together with eq.(8.10), allows Fig.9 to be drawn. This figure shows both the critical buckling stress curve of eq.(8.10) and the curves of the design bending stress for yield stresses of 52 and 36 ksi derived as indicated above.

It is apparent that when L/t < 200 for F_y = 52 and L/t < 300 for F_y = 36 ksi, F_b may be taken as ·66 F_y. This follows from the $F_o > 3\ F_y$ criterion used earlier.

Fig. 10 has been included to permit rapid estimation of F_b when the $\frac{L}{t}$ ratio and the yield stress are known. The maximum stress in a section may be determined directly from the applied moment and the section modulus.

9. Case III

The loading for Case III is shown in Fig. 3c. Since the moment is applied about the weak axis there is no possibility of buckling to a more stable configuration and the beam will continue to bend about this axis only. Therefore conventional beam formulas may be used. The maximum stress is given by:

$$\sigma_{max} = \frac{M_Y}{Z_Y} \quad —(9.1)$$

10. Loads not through the shear centre

Loads not through the shear centre will cause twisting of the angle section. Such loads will include the weight of the section acting through the centroid. These loads will cause an angle of twist given by:

$$\phi = \frac{TL^2}{8GK_T} \quad —(10.1)$$

For weight twisting, the value of T is:

$$T = \frac{wB}{4} \text{ in lb/in.}$$

where w = lb/in. length. The increased stresses due to additional twisting can be calculated from a generalised form of eq. (7.1).

$$\sigma = \frac{(M_v + \phi M_u)v}{I_v} - \frac{(M_u - \phi M_v)u}{I_u} \quad —(10.2)$$

A more exact and comprehensive solution to this problem can be found in Ref.20.

11. Case IV

The loading for Case IV is shown in Fig. 3d. In this case the moment can be resolved into moments about the U and V axes (principal axes) and the theory of Cases I and II applies.

More generally, if the applied moment acts in any position between the X or Y and U axes, the component moments M_x, M_u, resolved in the U, V directions, will produce stresses σ_x and σ_u. The design is satisfactory if:

$$\frac{\sigma_x}{F_x} + \frac{\sigma_u}{F_u} < 1 \quad —(11.1)$$

where F_x and F_u are the maximum permissible stresses associated with the axis under consideration.

12. Conclusions

It has been shown that for laterally unrestrained angle beams the following relationships apply:

Case I:

The stress at any point in the section is:

$$\sigma = \frac{3M}{B^2t}\left((V + 4U)\phi_t + V - 4U \right)$$

The maximum section stress is:

$$\sigma_{max} = \frac{3M(3 - \phi_t)}{\sqrt{2}B^2t}$$

where the angle of twist $\phi_t = \phi + \phi_o$.

If the maximum stress is calculated without resolving the applied load into U and V components, the result may be up to 50% less than the actual maximum stress. Twisting may be ignored if:

$$\sigma_a < \left(38 - \frac{1}{60} \cdot \frac{L}{t}\right) \text{ ksi.}$$

An alternative method of beam design for Case I is to consider the critical buckling moment given by:

$$\left[\frac{M_x}{Et^3}\right]_{cr} = \frac{\pi^2}{15} \cdot \frac{B^2}{Lt}\left[\left(\left(\frac{B^2}{Lt}\right)^2 + 0{\cdot}785\right)^{\frac{1}{2}} - \frac{B^2}{Lt}\right]$$

and then use Ref.7, Rule 5.4.3, to convert this into a design stress.

The values of L/t for which the safe bending stress, F_b, may be taken as $0{\cdot}66F_y$, are shown in Section 6.

Case II:

The angle of twist ϕ has no direct effect in this case and the safe bending stress can be calculated using 7, Rule 5.4.3, where the critical buckling stress F_o is obtained from:

$$F_o = \frac{\pi E}{2\sqrt{2{\cdot}6}} \cdot \frac{t}{L}$$

This may be ignored if $\frac{L}{t} < 200$ for F_y = 52 and $\frac{L}{t} < 300$ for F_y = 36 ksi, and a design stress of 0·66 F_y may be used.

Case III:
No secondary effects will occur and conventional beam formulas may be used.

Case IV:
The design is satisfactory if:

$$\frac{\sigma_x}{F_x} + \frac{\sigma_y}{F_y} < 1$$

where F_x and F_y are the appropriate maximum permissible stresses.

1. British Standards Institution, The Use of Structural Steel in Building BS 449, [illegible].
2. C. Marsh, Single Angle Members in Tension and Compression Proc. ASCE, 95 (ST5), May, [illegible], pp.[illegible].
3. L. Johnson, Practical Design Problems, Engineering Plasticity, Cambridge University Press, [illegible], pp.[illegible].
4. S. Mackey, An Experimental Investigation of the Behaviour of Mild Steel Compression Members in Light Lattice Frameworks. Structural Engineer, July, 1964, pp.150.
5. Task Committee on Tower Design, Electrical Transmission Line and Tower Design Guide Proc. ASCE, 93, (ST4), Aug., 1967, pp.245-282.
6. M. Finzi and G. Magenta, New Experiences During 8 Years of Tower Testing at the Lecco Station (Italy). CIGRE, [illegible], Session, Paper 22-03. (International Conference on Large Electrical Systems.)
7. Standards Association of Australia, Use of Steel in Structures, AS CA1.
8. Kerensky, O., Flint, A., and Brown, W, The Basis for the Design of Beams and Plate Girders in the Revised BS 153. Proc. ICE, 5 (Part 3), [illegible], pp.[illegible]-461.
9. Trahair, N. S., The Bending Stress Rules of the Draft AS CA1. JIE Aust., 38 (6), June, [illegible], pp. 131-141.
10. American Institute of Steel Construction (AISC), Specification for the Design Fabrication and Erection of Structural Steel for Buildings. AISC, New York.
11. Column Research Council, Design Criteria for Metal Compression Members. Wiley, N.Y., [illegible].
12. Lay, M. G., AS CA1–A Review and Explanation. Steel Construction, Aust. ISC, Special Issue, Spring, [illegible].
13. Lay, M. G., AS CA1 Design Guide. BHP Melb. Res. Lab. Report MRL 17/4A, [illegible]
14. BHP Co. Ltd., BHP-AIS Hot Rolled Carbon Steel Sections and Plates. BHP, [illegible].
15. Galambos, T. V., Structural Members and Frames. Prentice-Hall, N.Y., [illegible].
16. Bleich, F., Buckling Strength of Metal Structures. McGraw-Hill, 1952.
17. Massey, C., The Rotation Capacity of I Beams. British Welding Journal, Vol.[illegible], No.[illegible], Aug., [illegible].
18. Lay, M. G., Leigh, J., The Design of Laterally Unsupported Angles. BHP. Melb. Res. Lab. Rep. MRL 22/1.
19. Lay, M. G., The Basis for the Plastic Design Rules of AS CA1, Proc. 2nd Aust. Conf. Mech. of Materials and Structures, Adelaide, [illegible].
20. Trahair, N. S., Deformations of Geometrically Imperfect Beams, Proc. ASCE, 95 (ST7), July, [illegible], pp.[illegible].

Summary

The design criteria for angle beams can be summarised as follows:

Case	Use Simple Principal Axis Loading if:	Additional Effects if Column 2 Not Satisfied
I	(i) Stress Solution: $\sigma_e < 36 - \frac{1}{60} \cdot \frac{L}{t}$	$\sigma_{max} = \frac{2 \cdot 12M}{B^2t}(3 - \phi_1)$ (Fig.6)
	(ii) Critical Buckling Solution: See Table below.	Use $F_e \rightarrow F_{bc}$ conversion of Ref.7.
II	$\frac{L}{t} < 200$ ($F_y = 52$ ksi) $\frac{L}{t} < 300$ ($F_y = 36$ ksi)	Use Fig.10.
III	All Sections	—
Intermediate Loadings		$\frac{\sigma_x}{F_x} + \frac{\sigma_y}{F_y} < 1$

Critical Buckling Solution Case I:

Yield Stress F_y	B/t	Range for $F_{bc} = 0{\cdot}66F_y$
52	6	$0 < L/t < 680$
	11	$0 < L/t < 570$
	16	$0 < L/t < 330$
36	6	$0 < L/t < 990$
	11	$0 < L/t < 850$
	16	$0 < L/t < 690$

For other B/t values, interpolate.

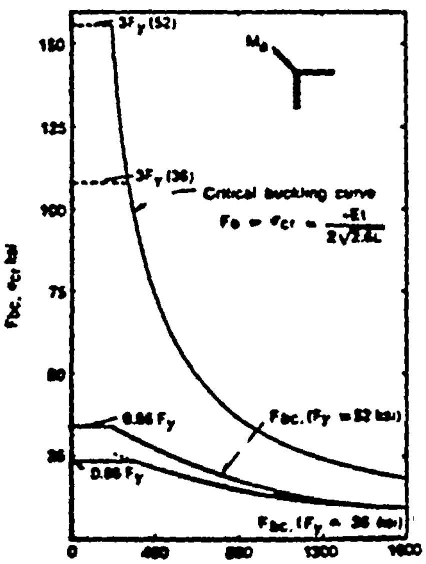

Fig.9. Critical buckling curve and curves for safe bending stress case II

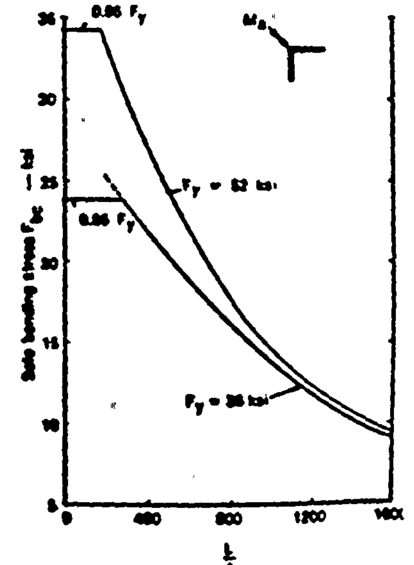

Fig.10 Graph for determination of F_{bc} for case II

The Behaviour of Laterally Unsupported Angles

By B. F. Thomas, J. M. Leigh, M.S., M.I.E.Aust. and M. G. Lay, B.C.E., M.Eng.Sc., Ph.D., F.I.E.Aust.*

Summary.—This paper reports the results of tests on laterally unsupported angles with equal and unequal legs subjected to a uniform moment over the entire laterally unsupported span. The moment is variously applied about the most common loading axes.

The results are compared with a theory proposed in earlier work. They show that the angle of twist, ϕ, normally reduces the maximum section stress produced. Since this twist has a significant influence on loading plane deflections, designers may safely use first order theory provided deflections do not exceed a typical limit of span/180.

The testing programme has also shown that practical angle sections are governed by stress and deflection criteria rather than by buckling.

LIST OF SYMBOLS†

B	Length of angle leg as defined in Fig. 1 $\left(\text{actual length} - \frac{t}{2}\right)$.
C	Centroid location.
E	Young's modulus.
F_y	Nominal yield stress.
F	Material yield stress.
F_e	Critical buckling stress.
I	Second moment of area about the axis perpendicular to the axis of load application.
L	Length of span.
M	Applied moment.
M_U	Component of the applied moment about the U-U axis.
M_V	Component of the applied moment about the V-V axis.
M^{cr}	Critical buckling moment.
Q	Length of angle leg as defined in Fig. 1 $\left(\text{actual length} - \frac{t}{2}\right)$.
S	Shear centre location.
UU	Major principal axis (U cross-section co-ordinate).
VV	Minor principal axis (V cross-section co-ordinate).
W	Polar axis.
X	Axis through the centroid parallel to the short angle leg.
Y	Axis through the centroid parallel to the long angle leg.
Z_a	Section modulus about the axis of load application.
t	Thickness of angle leg.
x	Deflection of the shear centre in the X-direction.
y	Deflection of the shear centre in the Y-direction.
σ_a	Nominal stress found from $\sigma_a = \dfrac{M}{Z_a}$.
σ_{max}	Actual maximum section stress.
ϕ	Angle of twist.
$\hat{\phi}$	Maximum angle of twist.
$'$	Differentiation with respect to w.
θ	Angle between the X and U axes (Fig. 1).

1.—INTRODUCTION

Most structural engineers are aware of the complex analysis involved in designing angle beams, if all the ramifications of their behaviour are to be taken into account. Common loading situations do not usually c[oin]cide with principal axes directions and such loading cases therefore [produ]ce biaxial bending deflections combined with axial twisting of the section. Structural design codes commonly (Refs. 1 and 2) give little or no design guidance for laterally unsupported angles and the 1968 SAA Steel Structures Code AS CA1 (Ref. 3) in Rule 5.4.3 stated:

> "The Standards Association of Australia is not prepared at this stage to make recommendations for angles which are not supported laterally."

This investigation, therefore, was aimed at developing a set of usable design formulae through a comprehensive testing programme.

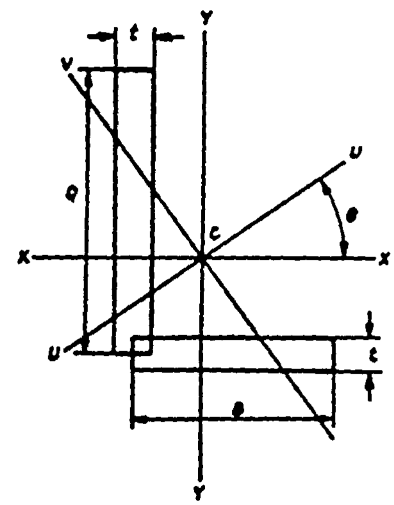

Fig. 1.—Simplified Angle Section Dimensions and Locations of Axes.

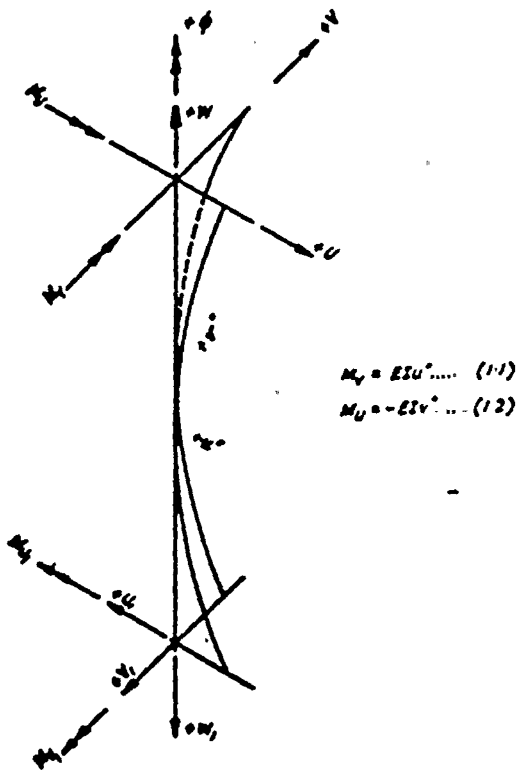

NOTE -
AXES ARE DRAWN WITH W OR W, AS THE OUTWARD DRAWN NORMAL FROM THE SURFACE UNDER CONSIDERATION.

Fig. 2.—Sign Convention.

*Paper No. 3197, submitted by the authors on June 7, 1972.

Mr Thomas is an Experimental Officer, Product Engineering Department, BHP Research Laboratories, Melbourne.

Mr Leigh is a Research Officer, BHP Research Laboratories, Melbourne.

Dr Lay is Senior Principal Research Officer, BHP Research Laboratories, Melbourne.

†This notation is coupled with the sign convention given in Fig. 2.

During the initial stages of the programme a general theory describing the elastic behaviour of thin walled sections (Ref. 4) was used to determine the important parameters which governed the behaviour of equal angles (Ref. 5). The design rules proposed as a result of this study permitted a more enlightened approach to the experimental work.

The theory was subsequently developed into general design rules covering all angle sections (Ref. 6) and this permitted the compilation of safe load tables for angle beams (Ref. 7). Since the testing programme proceeded in parallel with the theoretical analysis, it was possible to make progressive comparisons between the results of both sections of the work.

The loading rig, which is described in Section 4.1, was designed to apply a uniform moment to a beam laterally unrestrained between two torsional restraint points. This loading constituted the most critical buckling situation (Ref. 8) in accordance with the other buckling rules of CA1 (Refs. 9 and 10). Test specimens included both equal and unequal angles loaded about axes parallel to one leg.

Although the project was primarily concerned with the elastic behaviour of angle beams, a number of failure tests were also carried out to determine the ultimate load carrying capacity and failure modes of these sections.

2.—LOADING CASES

The loading cases considered (Fig. 3) represent the most common loading conditions for angle beams. These are:

2.1 Equal Angles:

Case I—Moment applied about an axis parallel to either the X-X or the Y-Y axis.

2.2 Unequal Angles:

Case I—Moment applied about an axis parallel to the Y-Y axis, that is, parallel to the long leg.

Case II—Moment applied about an axis parallel to the X-X axis, that is, parallel to the short leg.

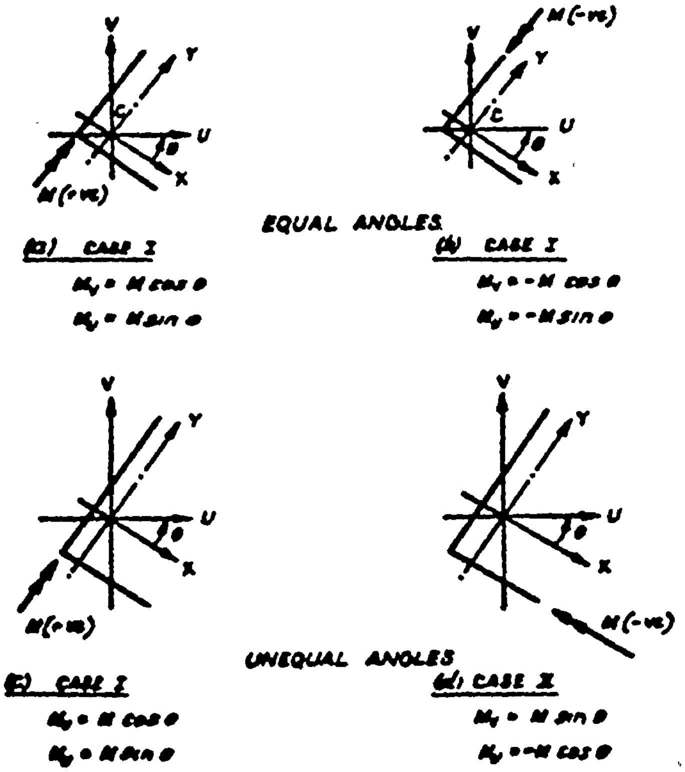

Fig. 3.—Loading Cases.

3.—TESTING PROGRAMME

The parameter which has the most pronounced influence on the lateral stability of angle sections is $\frac{B+Q}{2t}$. The effect of this parameter is demonstrated by the critical buckling analysis for equal angles (Ref. 5) which shows that for Case I loading the critical buckling moment is a function of B/t (analogous to $\frac{B+Q}{2t}$ for unequal angles) and L/t. If failure stresses are to remain unaffected by elastic buckling (Refs. 10 and 12) the value of L/t for a given $\frac{B}{t}$ ratio must be within the range given by Table I.

TABLE I

Elastic Buckling Effects of Various Angle Sections (36 ksi Steel)

Yield Stress	$\frac{B}{t}$	Range for No Elastic Buckling Effects
$F_y = 36$ ksi	6	$0 < \frac{L}{t} < 990$
	11	$0 < \frac{L}{t} < 850$
	16	$0 < \frac{L}{t} < 690$

The table shows that sections with the practical upper limit B/t of 16 have less buckling resistance than sections with a lower value.

This criterion was used for selecting the sections tested. Both equal and unequal angles were tested and the values of B/t for each section are given in Table II, which also summarises the testing programme.

A single specimen was used for each series. This was made possible by testing the longer lengths first and keeping the stresses below yield, until a "destruction" test was required.

TABLE II

Testing Programme Summary

Test No.	Section Dimensions	$\frac{B+Q}{2t}$	$\frac{L}{t}$	Loading Case	Applied Moment Sense
EA2	3" × 3" × 0.187"	16	1600	Case I	+
EA3	3" × 3" × 0.187"		1600	Case I	−
EA4	3" × 3" × 0.187"		1200	Case I	+
EA5	3" × 3" × 0.187"		1200	Case I	−
EA6	3" × 3" × 0.187"		800	Case I	+
EA7	3" × 3" × 0.187"		800	Case I	−
EA8	3" × 3" × 0.187"		400	Case I	+
UE1	2.5" × 2" × 0.25"	16	1200	Case II	−
UE2	2.5" × 2" × 0.25"		1200	Case I	+
UE5	2.5" × 2" × 0.25"		1200	Case I	Follow-up test to failure after UE2. Always referred to as UE2 in text.
UE6	2.5" × 2" × 0.25"		400	Case I	+
UE7	2.5" × 2" × 0.25"		400	Case II	−
UE3	3.5" × 2.5" × 0.187"	9	1600	Case I	+
UE4	3.5" × 2.5" × 0.187"		1600	Case II	−
UE8	3.5" × 2.5" × 0.187"		400	Case II	−
UE9	3.5" × 2.5" × 0.187"		400	Case I	+

4.—EXPERIMENTAL APPARATUS

4.1 Loading Rig:

The purpose of the loading rig was to apply a uniform loading moment to an angle test specimen while applying only torsional restraint and vertical support at the ends, i.e. $\phi = \phi'' = 0$ at both ends. Spherical joints were used where necessary to ensure that the load application did not provide lateral restraint to the test piece. The loading beam thus reacted horizontally and vertically with the test specimen and only applied moments in a vertical plane parallel to the angle at the support. It was not in any way connected to the floor.

The rig comprised two independent, identical assemblies which could be positioned on the loading floor at any required distance to accommodate changes in the test length. Each assembly consisted of a stand surmounted by a roller bearing, for vertical support, and a frame which housed adjustable horizontal restraint supports which had additional function of providing torsional restraint to the ends of a beam being tested.

The addition of weights to the loading beam produced a force in the vertical link which was connected to the end of the test piece. The loading beam was supported by a needle roller bearing in the vertical link which ensured that the vertical link would always locate normal to the loading beam, whatever its position. The assembled rig is shown pictorially in Fig. 5. Detailed drawings of the rig are given in Ref. 16.

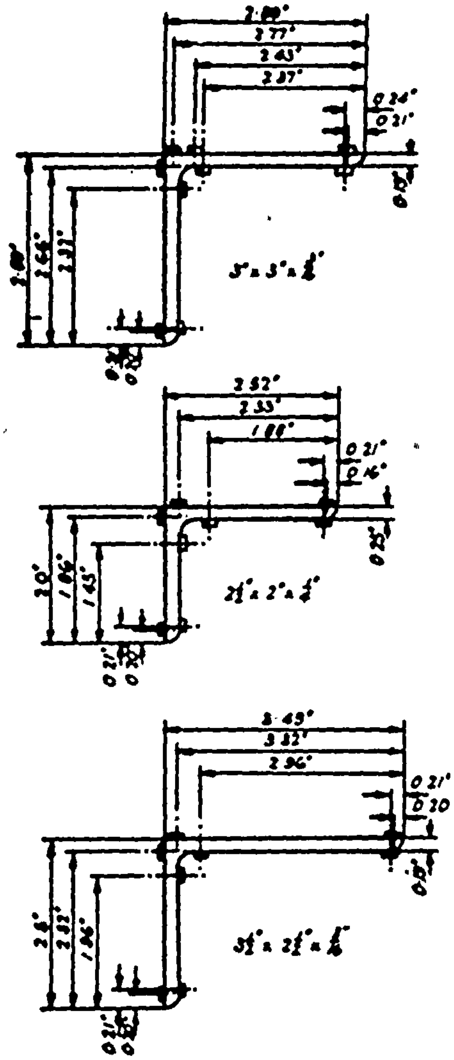

Fig. 4.—Strain Gauge Locations.

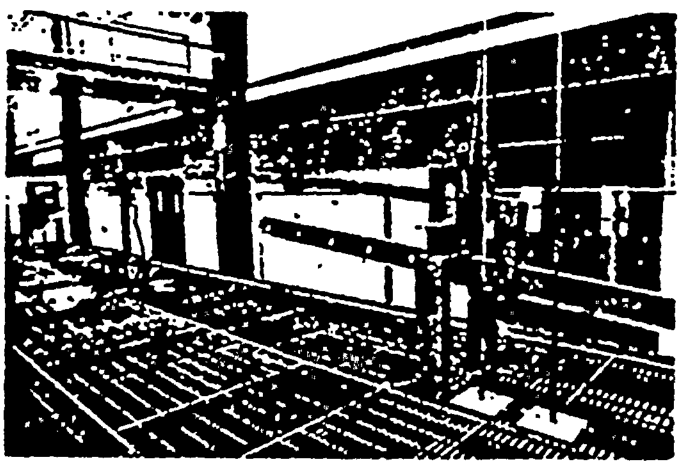

Fig. 5.—Assembled Rig.

4.2 Measuring Instruments:

stations were measured by the optical lever principle using a sim... mirror system. This system also avoided the introduction of specimen restraints. The maximum value of the angle of twist (ϕ_{max}) was also measured at mid-span using a bevel protractor. Vertical loading plane deflections were measured at mid-span and quarter points by means of a theodolite and graduated scale. Horizontal deflections were measured with a steel tape.

A number of strain gauges were placed on the section at its mid-span position (Fig. 4). The gauges were read using an automatic data logging system (Ref. 11) which converted the readings directly to stress values. By following the testing programme outlined earlier, it was possible to use the one set of strain gauges for a complete series of tests.

5.—TENSILE TESTS

Tension tests were carried out on coupons obtained from each angle section tested. The tests were performed on an Instron Universal testing machine with a crosshead speed of 0.079 inch/min which corresponds to a strain rate of 0.005 min^{-1}. Average values of material yield stress and tensile stress were found and these indicate that the material conformed to the requirements of AS A149 (Ref. 14).

6.—RESULTS

6.1 Stress Levels:

Stress values were measured at mid-span using strain gauges located as shown in Fig. 4. The nominal section stress has been used as a yardstick for comparison with the maximum section stress σ_{max} which occurred at mid-span at the tip of the vertical leg. The maximum (flange tip) stress was determined by linear extrapolation from the stress distribution across the section. The nominal stress can be found from

$$\sigma_a = \frac{M}{Z_a}$$

where M is the applied moment and Z_a is the section modulus about the axis of load application.

Figs. 6 and 7 show curves describing the relationship between σ_a and σ_{max} for

(*a*) Tests results.

(*b*) Theory with zero angle of twist ($\phi = 0$).

(*c*) Theory with $\phi \neq 0$.

(*d*) Theory with measured test values of ϕ.

Fig. 6 includes the results of tests on the 3" × 3" × 3/16" section with an L/t ratio of 1600. This section was subjected to applied moments in a positive (EA2) and negative (EA3) sense about an axis parallel to one leg.

For the same applied load the stress levels recorded were up to 15% greater for a loading sense which produced tensile stresses in the horizontal leg (EA2). This difference was only 4% at a stress level of $0.66F_y$ where F_y is the nominal yield stress (36 ksi). Hence within the design range the difference in behaviour for reversed loading sense is negligible.

The difference results from the fact that the constitutive equations (Refs. 5 and 6) were based on small deflections theory whereas in fact for large spans, mid-span loading plane deflections were in the order of 12 inches. Since deflections of this magnitude are not experienced in practice, and since small deflection theory conservatively predicts angle behaviour where deflections exceed a limit of span/180, a more refined analysis is not justified.

The unequal angles tested (Fig. 7) behaved in a similar manner for both Cases I and II. For all sections, tests on shorter lengths (EA6, EA7, EA8, UE6, UE7, UE8, UE9) indicated close agreement with the theory.

Fig. 8 shows a typical stress distribution of the sections tested for points which lie closest to stress levels of $0.66F_y$ and F_y.

Fig. 7 (tests UE2, UE4) show the two buckling failures which occurred before the full material yield stress was reached. These failures are discussed further in Section 6.3. For all tests the theoretical and experimental stress values were in good agreement up to a maximum section stress of $0.66F_y$. Beyond this level, for beams with large values of L/t the predictions of first order theory (i.e. assuming $\phi = 0$) were conservative. Therefore, the simple no-twist relationship (Refs. 5 and 6)

$$\sigma_{max} = 1.25\ \sigma_a$$

should give conservative results at all stress levels.

6.2 Angles of Twist ϕ_{max}:

Angles which are loaded about axes other than principal axes will twist axially to align the weak principal axis with the axis of load application. This twist in the test series was measured at mid-span and recorded values are compared with the theoretical predictions in Fig. 9 for all sections tested. Points A and B coincide with nearest attainment of $0.66F_y$ and F_y level stresses. In each case the direction of load application opposed the dead weight load, hence initial twisting due to the dead weight of the beam was reduced as the beam was loaded. The zero twist position, therefore, corresponded approximately with the condition when the applied load effect equalled the dead weight load. This load has been taken as the starting point for plotting the theoretically predicted values of angle of twist (ϕ_{max}) (Ref. 6).

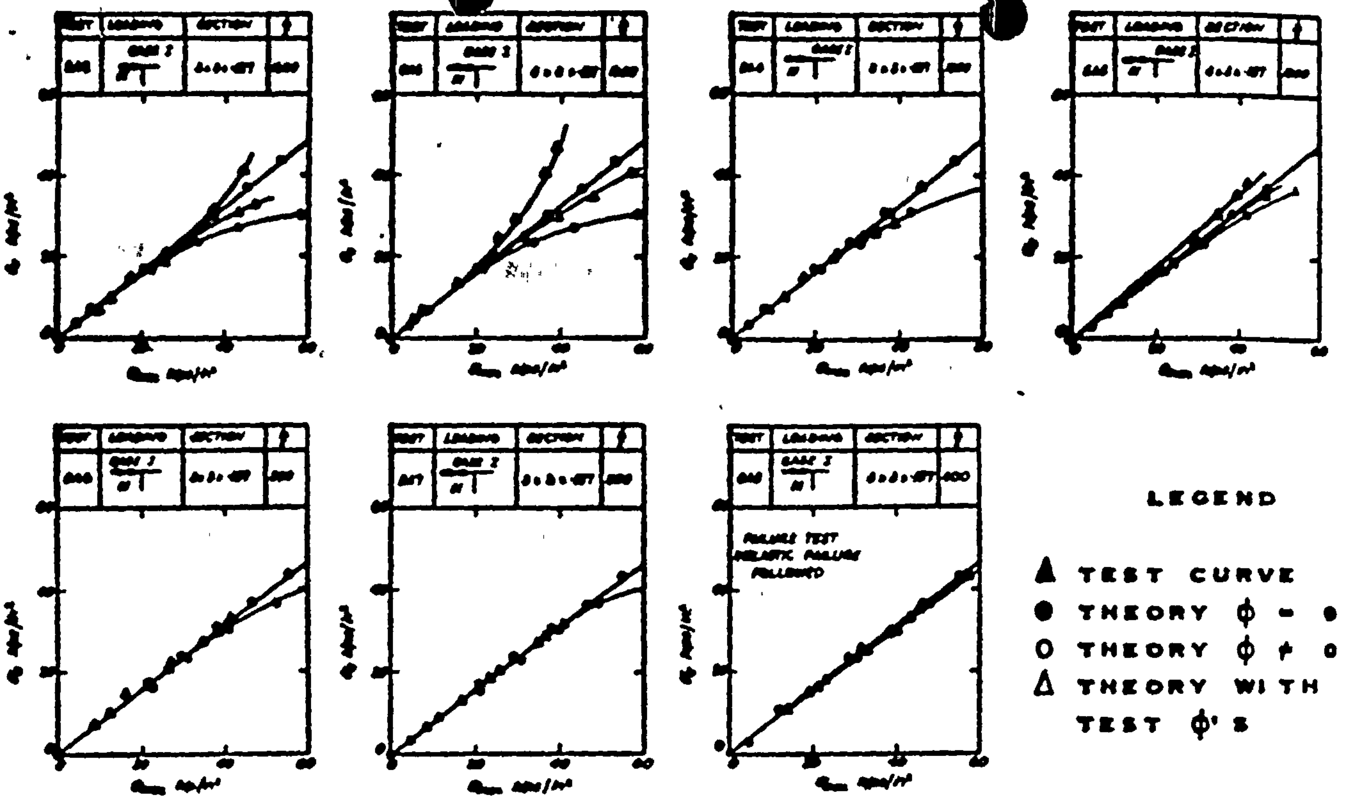

Fig. 6.—Relationship between Nominal Applied Stress σ_a and Maximum Stress σ_{max} for Tests on Equal Angle Sections.

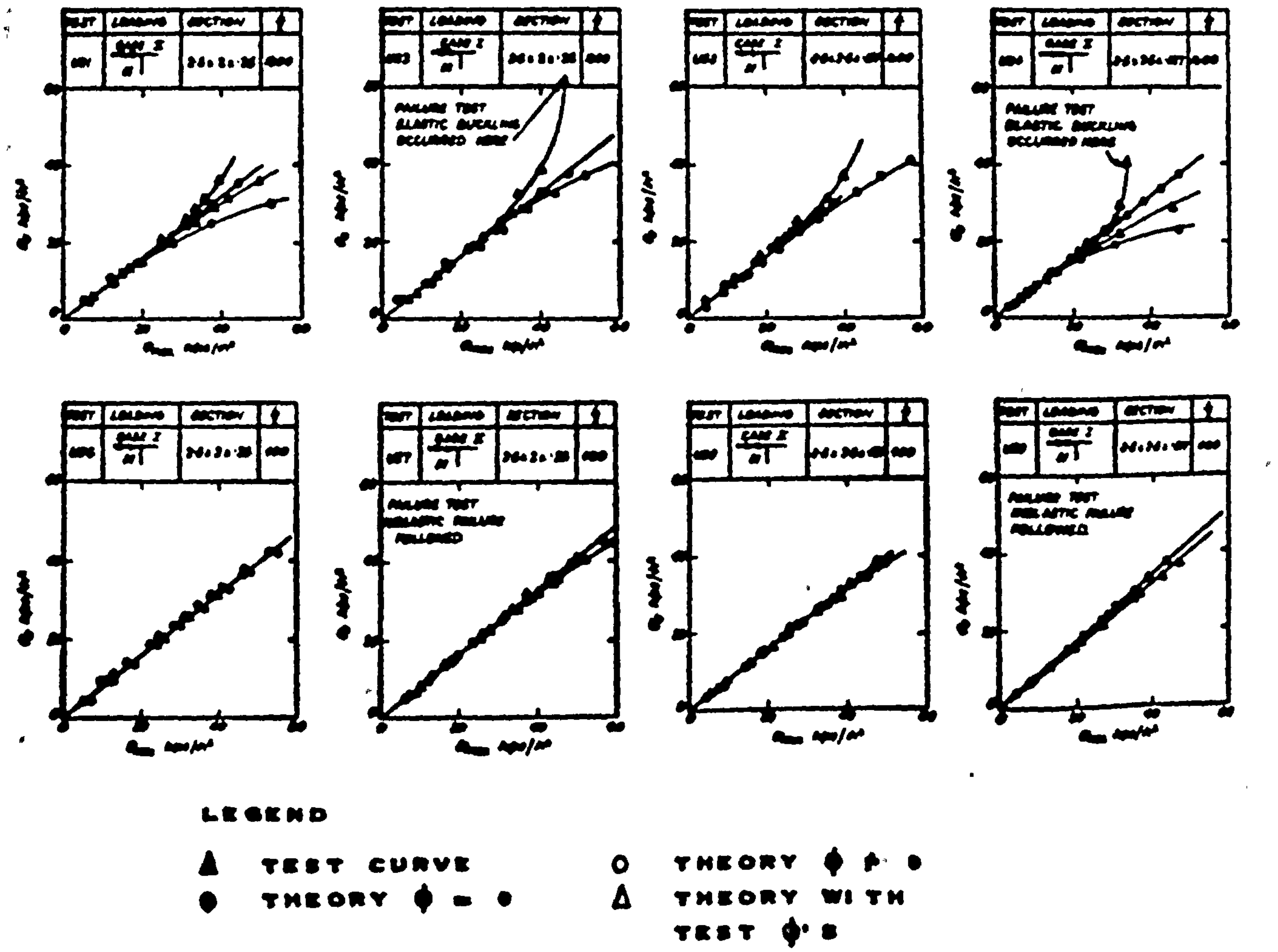

Fig. 7.—Relationship between Nominal Applied Stress σ_a and Maximum Stress σ_{max} for Tests on Unequal Angle Sections.

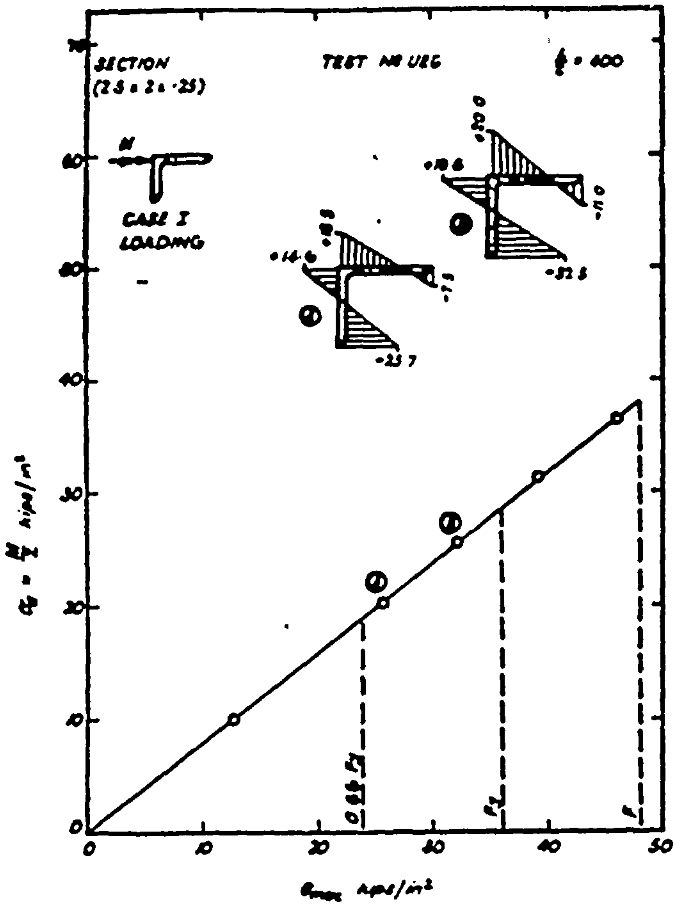

Fig. 8.—*Relationship between Nominal Applied Stress σ_a and Maximum Section Stress σ_{max} for Test No. UE6.*

The curves of Fig. 9 (tests UE1, UE2, UE3, UE4, EA2, EA3) are consistent with the stress curves of Fig. 7 (same tests) in that they show graphically the torsional stiffening which takes place at large values of applied load and correspondingly large angles of twist. This effect is less significant for shorter lengths, consequently theoretical and experimental results are in closer agreement (Fig. 9—tests UE6, UE7, UE8, UE9, EA6, EA7). Sections subjected to Case II loading must twist through an angle of $(90-\theta)°$ to align with the minimum principal axis where θ is the angle between the X and U axes, whilst Case I loading requires only a twist through $\theta°$. This is reflected in the large angles of twist recorded for Case II loadings (Fig. 9—tests UE1, UE4, UE7).

6.3 Tests to Failure:

Five tests to failure were performed on both equal and unequal angles for a variety of L/t values. These tests are summarised in Table III which also shows the value of the applied moment at which failure occurred and failure modes. In all cases failure occurred at the end of supports.

TABLE III

Summary of Failure Test Results

Test No.	Section	$\frac{L}{t}$	Loading Case	Failure Moment (kips-in)	Failure Mode
EA8	3" × 3" × 0.187"	400	I	20.5	Torsional Buckling
UE4	3.5" × 2.5" × 0.187"	1600	II	22.0	Torsional Buckling
UE9	3.5" × 2.5" × 0.187"	400	I	19.2	Torsional Buckling
UE2	2.5" × 2" × 0.25"	1200	I	15.7	Flexural Buckling
UE7	2.5" × 2" × 0.25"	400	II	18.9	Torsional

Fig. 10 shows the relationship between the critical buckling curve and design curve for each of the unequal angle failure tests. The critical buckling curve is obtained from the analysis given in Ref. 16 and the design curve can be found using Rule 5.4.3 of CA1 (Ref. 3). The horizontal line, denoted $3F_y$, represents the value of $\frac{M^{cr}}{Et^3}$ to produce a stress of $3F_y$ where F_y is the nominal yield stress (36 ksi). It is normally assumed (Refs. 10 and 12) that failure stresses will be unaffected by elastic buckling if the buckling stress is at least three times the material yield stress. All sections tested behaved in accordance with this assumption. The elastic buckling failure (test UE4) plots to the right of the intersection of the critical buckling curve and the $3F_y$ line, i.e. $F_e < 3F_y$. The actual failure moment was somewhat greater than that predicted by the critical buckling analysis, due probably to higher order effects for this very " slender " case.

Elastic buckling also occurred in test UE2 at a critical moment corresponding to the theoretically predicted value for this less " slender " case. The sections of tests UE9 and UE7 obtained full yield stress before failure. Good agreement with the $3F_y$ assumption is apparent from Fig. 9 (tests UE7, UE9) which show that the failure points plot within the region expected for inelastic buckling. The results for the equal angle test (EA8) have not been graphed since failure occurred inelastically in agreement with similar failures on the unequal angles tested.

6.4 Deflections:

Biaxial bending deflections resulting from non-principal axis loading were measured as shear centre displacements in the loading plane and normal to the loading plane. Fig. 11 includes the recorded results, for the section 3" × 3" × 0.187" loaded as shown in Fig. 3(*a*), compared with the predicted curves for both first and second order theory ($\phi = 0, \phi \neq 0$) for a variety of L/t ratios.

This limit is recommended by CA1 for structural applications where angles could be used. Beyond this level, for $L/t > 1000$, second order theory conservatively predicted the loading plane deflections whereas first order theory under-estimated this deflection by up to 20%.

Similar results were obtained for the reverse loading case and for unequal angles with Case II loadings (Fig. 11—tests UE1, UE4, UE7, UE8). Unequal angles with Case I loading and $L/t > 1000$ deflected less than predicted by either first or second order theory for load values which caused deflections in excess of $L/180$ (Fig. 11—tests UE2, UE3).

The tests indicate that provided deflections are limited to $L/180$, first order theory will give an accurate estimate of the loading plane deflection. Consequently, if it is desired to use sections which develop the full bending stress of $\sigma_{max} = 0.66F_y$, then the use of the design formula (Refs. 5 and 6)

$$\frac{L}{B+Q} < \frac{600}{F_y}$$

will permit the attainment of full stresses and avoid lateral buckling problems. Above this limit the use of second order theory will ensure that results are conservative for all cases.

CONCLUSIONS

A total of 15 tests were performed on laterally unsupported angles with equal and unequal leg lengths for a variety of L/t values. The loading condition was a uniform moment over the entire laterally unsupported span and this load was applied about an axis parallel to an angle leg. Uniform moment is the most critical design situation. Adjustments for other loadings would probably follow standard procedures (Refs. 4 and 8), however this was not studied in the present work. The solutions given will always be conservative.

From the results of these tests it was concluded that for the loading conditions stated above:

1. The angle of twist (ϕ) causes a reduction in the maximum section stress produced. Therefore, first order theory gives a conservative estimate of this stress, i.e.

$$\sigma_{max} = 1.25\ \sigma_a$$

2. The angle of twist (ϕ) has a significant influence on the maximum loading plane deflection beyond a deflection of $L/180$ and second order theory gives a conservative estimate of deflection above this level.
3. The five tests to failure indicated that laterally unsupported angles will be unaffected by elastic buckling provided that the critical buckling stress is at least three times the material yield stress.
4. Practical angle sections are seen to be governed by stress or deflection limitations rather than by buckling.

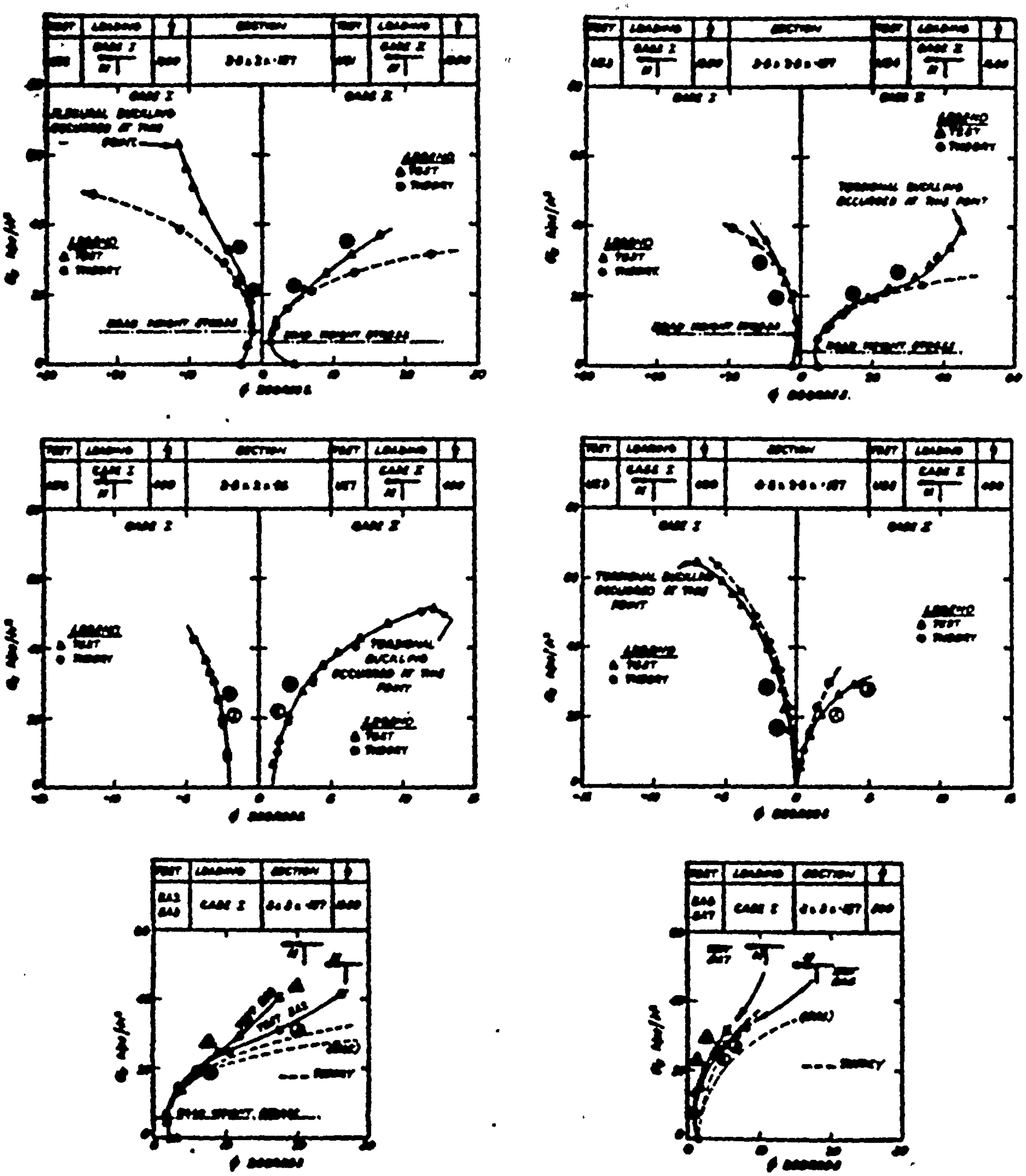

Fig. 9.—Relationship between Nominal Applied Stress σ_o and Maximum Angle of Twist ϕ.

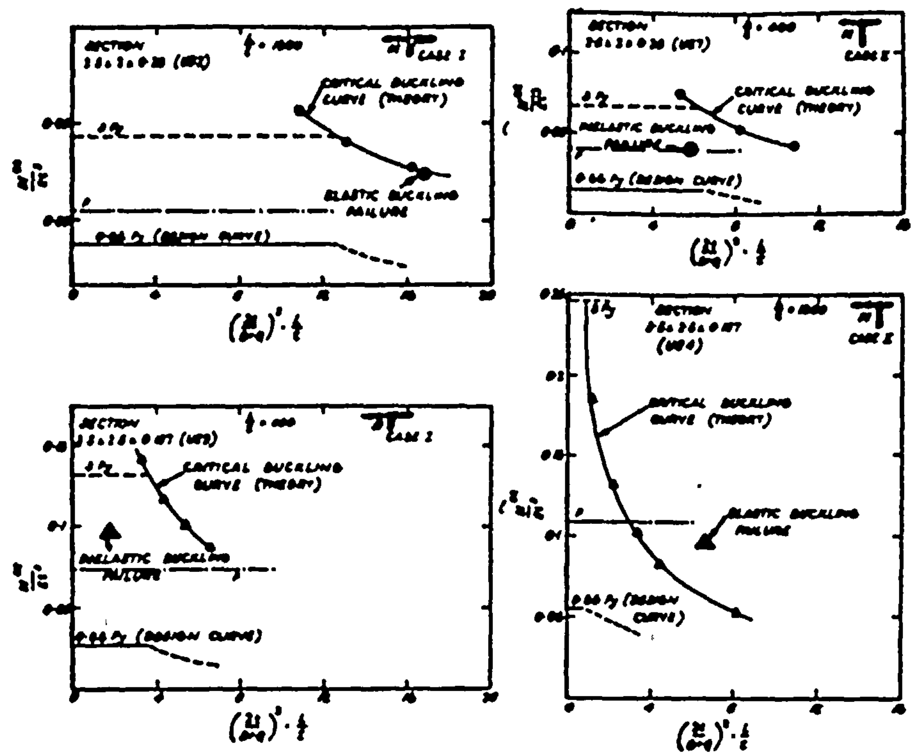

Fig. 10.—Test to Failure Results Compared with Critical Buckling Curves and Design Curves.

References

1. British Standards Institution—*The Use of Structural Steel in Buildings.* BS 449—1959.

2. American Institute of Steel Construction (AISC)—*Specification for the Design, Fabrication and Erection of Structural Steel for Buildings.* New York, AISC, 1969.

3. Standards Association of Australia—*Use of Steel in Structures.* AS CA1—1968.

4. Galambos, T. V.—*Structural Members and Frames.* New York, Prentice-Hall, 1968.

5. Leigh, J. M. and Lay, M. G.—The Design of Laterally Unsupported Angles. *BHP Tech. Bulletin,* Vol. 13, No. 3, Nov., 1969.

6. Leigh, J. M. and Lay, M. G.—Laterally Unsupported Angles with Equal and Unequal Legs. *BHP Melb. Research Lab. Report MRL* 22/2, July, 1970.

7. Leigh, J. M. and Lay, M. G.—Safe Load Tables for Laterally Unsupported Angles. *BHP Melb. Research Lab. Report MRL* 22/3, Nov., 1970.

8. Column Research Council—*Design Criteria for Metal Compression Members.* New York, Wiley, 1966.

9. Lay, M. G.—AS CA1—A Review and Explanation. *AISC Steel Construction,* Special Issue, 1968.

10. Lay, M. G.—AS CA1 Design Guide. *BHP Melb. Research Lab. Report MRL* 17/4D, 1971.

11. Thomas, B. F. and Knight, D. C.—Data Acquisition at the Melbourne Research Laboratories. *BHP Melb. Research Lab. Report MRL* A4/3, Oct., 1971.

12. Lay, M. G.—The Basis for the Plastic Design Rules of AS CA1. *Proc. Second Australasian Conf. Mechanics of Structures and Materials, Adelaide,* 1969.

13. Farwell, C. R. and Galambos, T. V.—Non-uniform Torsion of Steel Beams in Inelastic Range. *Proc. ASCE, Jour. Structural Div.,* Vol. 95, No. ST12, Dec., 1969, pp. 2813-29.

14. Standards Association of Australia—*Mild Steel for General Structural Purposes.* AS A149—1965.

15. Broken Hill Pty Co. Ltd—*BHP-AIS Hot Rolled Carbon Steel Sections and Plates,* 1969.

16. Thomas, B. F. and Leigh, J. M.—Behaviour of Laterally Unsupported Angles. *BHP Melb. Research Lab. Report MRL* 22/4, Dec., 1970.

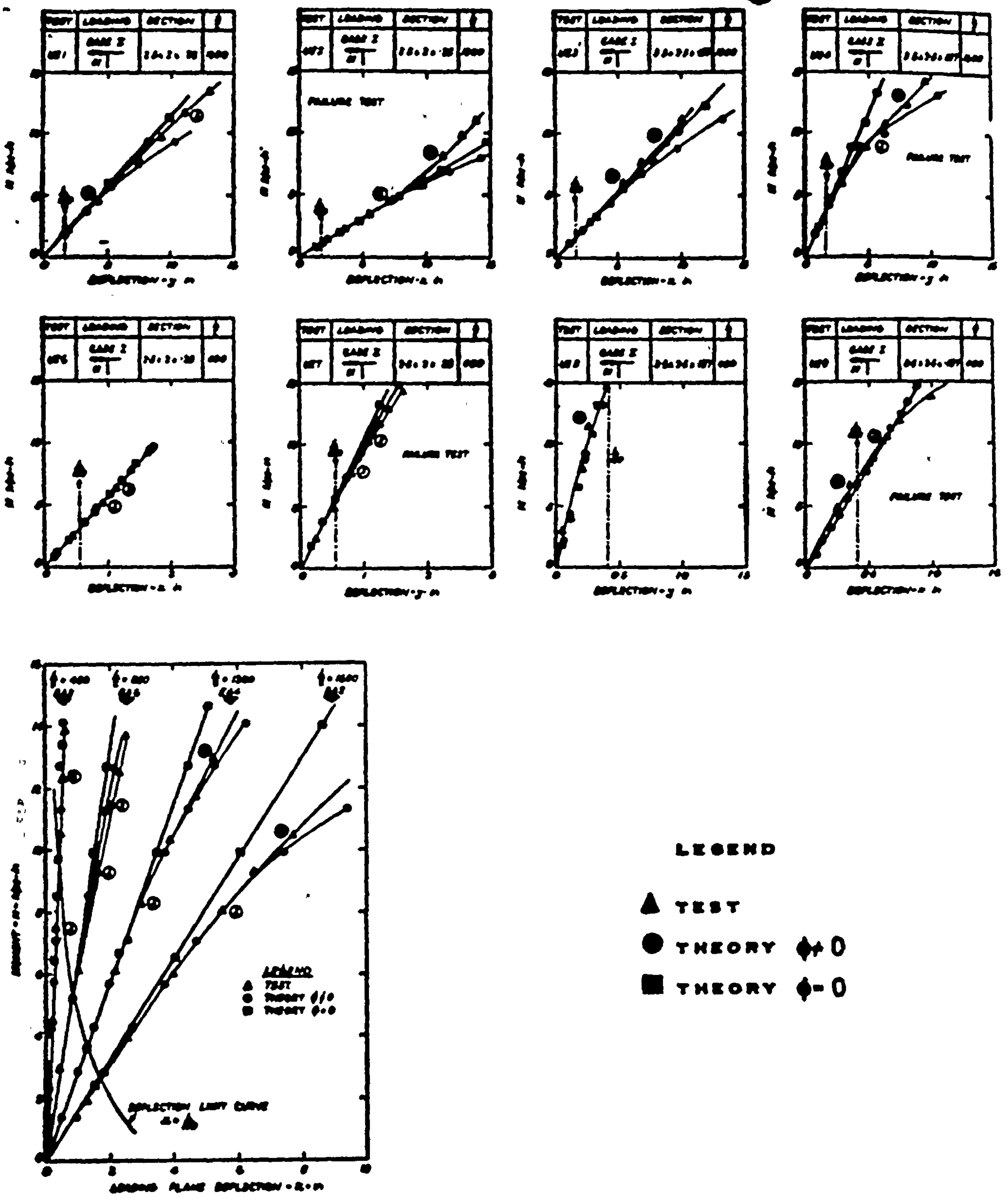

Fig. 11.—Relationship between Applied Moment M and Maximum Loading Plane Deflections.